frontiers in Earth Science

ORIGINAL RESEARCH
published: 13 June 2018
doi: 10.3389/feart.2018.00078

Correlated Changes Between Volcanic Structures and Magma Composition in the Faial Volcanic System, Azores

René H. W. Romer[1], Christoph Beier[1], Karsten M. Haase[1] and Christian Hübscher[2]*

[1] GeoZentrum Nordbayern, Friedrich-Alexander-Universität Erlangen-Nürnberg, Erlangen, Germany, [2] Center for Earth System Research and Sustainability, Institut für Geophysik, Universität Hamburg, Hamburg, Germany

OPEN ACCESS

Edited by:
Adriano Pimentel, Centro de Informação e Vigilância Sismovulcânica dos Açores (CIVISA), Portugal

Reviewed by:
David A. Neave, Leibniz Universität Hannover, Germany
Valerio Acocella, Università degli Studi Roma Tre, Italy
Ralf Gertisser, Keele University, United Kingdom

***Correspondence:**
René H. W. Romer
rene.romer@fau.de

Specialty section:
This article was submitted to Volcanology, a section of the journal Frontiers in Earth Science

Received: *26 January 2018*
Accepted: *25 May 2018*
Published: *13 June 2018*

Citation:
Romer RHW, Beier C, Haase KM and Hübscher C (2018) Correlated Changes Between Volcanic Structures and Magma Composition in the Faial Volcanic System, Azores. Front. Earth Sci. 6:78. doi: 10.3389/feart.2018.00078

The interaction between magmatic and tectonic processes in ocean intraplate volcanism yields insights into the ascent and transport of magmas. Many oceanic intraplate studies lack a temporal component and do not consider changes in tectonic regime and/or magmatic processes during the evolution of magmatic systems. The eastern part of the Azores archipelago formed under the influence of both an intraplate melting anomaly and a system of ultraslow spreading rift axes. The majority of recent submarine and subaerial eruptions in the Azores occur along volcanic rift zones and thus melt transport and volcanic processes are largely controlled by tectonic processes, and are therefore ideally suited to study volcano-tectonic interactions. Here, we investigate how variable the magmatic and tectonic processes are in space and time and how they interact. We present new bathymetric, geophysical, geochemical, and Sr-Nd-Pb isotope data from Faial Island and the surrounding seafloor, providing insights into the interaction between the asthenospheric melting anomaly and extensional lithospheric stresses. The bathymetry reveals large submarine volcanic rift zones on the western flank of Faial, including that of the 1957–1958 Capelinhos eruption. Based on absolute ages and seismic imagery, we develop a relative chronology of the magmatic evolution of the submarine rift zones. Their preferred WNW-ESE orientation implies that the stress field has not changed within the last ∼1 Ma. We can however show that melt productivity progressively decreased with time. Compositionally different magma batches fed distinct volcanic rift zones and edifices, suggesting that changes in the melting regime occur on a small spatial scale and that the distribution of compositionally similar lavas is tectonically controlled. As melt supply decreases, the tectonic influence on volcanism increases with a stronger localisation of melts along tectonically controlled lineaments. The youngest mafic and intermediate melts (<10 ka) on Faial are exclusively erupted along single rift zones and cover a smaller area, whereas the older volcanism was more widespread.

Keywords: oceanic intraplate volcanism, tectonic stress, lithospheric extension, rift zones, melt transport, dyking

INTRODUCTION

Volcanoes situated close to plate boundaries form by the interaction between magmatic intraplate processes and those associated with the tectonic stress field. Tectonic and magmatic processes both affect melt formation, ascent, movement in the shallow crust, and finally eruption. For example, volcanoes at oceanic spreading axes are commonly elongated reflecting the intrusion of kilometer long dikes above which lavas erupt and build up volcanic ridges (Morgan, 1987). Studies of oceanic island volcanoes, e.g., Hawaii, Iceland, and the Canary Islands, have shown that extensional forces on different local and regional scales generate lithospheric pathways for the ascending melts (Garcia et al., 1996; Klügel et al., 2005a; Gudmundsson et al., 2014). However, little is known on how structural features or compositions of magmas change if an extensional component is present as a response to either changes in melting or tectonic regime. If volcanism is predominantly concentrated along rift zones, melting rates and pathways of magma transport are strongly controlled by lithospheric extension (Galipp et al., 2006). Shorttle et al. (2013) show that magmas appear to be related to each other on length scales similar to those of individual, rift-parallel volcanic systems, implying that extension may impart some control on the development of segmentation.

The eruption of melts in intraplate environments generally produces alkaline basalts that display enriched trace element and isotope signatures (White et al., 1976; Zindler and Hart, 1986; Hofmann, 1997) and may be ideally suited to investigate the extent of mantle heterogeneity (Hofmann, 2003; Stracke, 2012). The formation of melts in intraplate environments has generally been attributed to either increased temperatures (Morgan, 1971; Schilling, 1975; White et al., 1976; Cannat et al., 1999) or increased volatile contents (Schilling et al., 1980; Bonatti, 1990) or a combination of these. Contrarily, melt formation at oceanic spreading axes frequently results from adiabatic decompression melting by the upwelling depleted upper mantle (McKenzie and Bickle, 1988). Melts that have formed in an intraplate environment from melting of an enriched mantle rising beneath an extensional regime, e.g., in the Azores, may provide a means to disentangle the processes influencing the final melt composition and those that influence the tectonic stress field and the structure of related volcanic bodies. Studies on ocean islands generally either deal with the volcanic evolution of the islands (e.g., in the Azores; Larrea et al., 2014) or the tectonic evolution of a particular system or area (e.g., Hildenbrand et al., 2014; Miranda et al., 2018), or a combination of both (e.g., on Faial, Trippanera et al., 2014). Yet, most of these studies do not consider the temporal and spatial evolution within a single magmatic system. In many intraoceanic systems these processes are however linked, i.e., tectonic stresses may affect volcanic processes. The variability in the temporal evolution of a single volcanic system and how and whether changes in either tectonic regime or melting conditions are reflected in the respective structural and compositional features remains however unknown.

Our main aim is to investigate how magma compositions and eruption patterns evolve at ocean volcanoes in space and time. The Azores submarine volcanic systems and islands are strongly influenced by extension of the lithosphere above a mantle melting anomaly (Gente et al., 2003; Vogt and Jung, 2004; Beier et al., 2008) making them an ideal target location for studying volcano-tectonic interactions. The boundary between the Eurasian, African and American lithospheric plates has experienced significant tectonic changes in the past 10 Ma (Miranda et al., 2018; Vogt and Jung, 2018). During this period the magmatism and the tectonic stress are probably an omnipresent feature in the Azores allowing to determine the impact of the structural regime on intraplate melting.

Here, we combine new bathymetric data with geochemical and petrological data from a series of subaerial and submarine mafic to intermediate igneous rock samples from Faial and the north- and southwestern submarine ridges extending from the island. We expand existing chemical and structural studies of the island toward the submarine volcanic edifices in order to reconstruct the volcanic evolution of Faial and the surrounding submarine structures. We show that much of the temporal evolution of melts on timescales >1 Ma are controlled by mantle melting processes, in which changes in degree of partial melting and enrichment result in geochemically distinct lavas. The tectonic control on the volcanism becomes more significant as mantle processes, i.e., the degree of partial melting and the mantle source, progressively change. Our observations may also be applicable to other smaller volcanic rift systems and indicate that mantle heterogeneity and extensional movements can impact on the composition and ascent of melts on different temporal and spatial length scales.

GEOLOGICAL SETTING

The Azores Plateau in the Central Northern Atlantic is separated by the Mid-Atlantic Ridge (MAR) into an eastern and western part (**Figure 1**). Six of the seven islands in the eastern part of the archipelago are influenced by the NW-SE striking Terceira Rift or its predecessors, only Santa Maria displays no substantial rift component. The Terceira Rift is an ultraslow oblique spreading axis that formed about 1 Ma ago (Vogt and Jung, 2004). The Terceira Rift and the MAR form the ridge-ridge-ridge triple junction located either west of Faial and/or Graciosa (Grimison and Chen, 1988). The easternmost island Santa Maria and the eastern part of São Miguel are related to the W-E striking East Azores Fracture Zone (EAFZ) which is the former boundary between the African and Eurasian plate (Luis et al., 1994). Three of the seven volcanic islands and an active seamount in the eastern plateau (São Miguel, Terceira, Graciosa, and João de Castro seamount) are located along the recently active Terceira Rift, divided by deep non-volcanic basins (Beier et al., 2008). Three islands south of the Terceira Rift (e.g., Faial, Pico, São Jorge) may also be related to a previous rifting movement (Vogt and Jung, 2004), forming parallel lineaments relative to the nowadays position of the Terceira Rift (Beier et al., 2015). They thus represent former extinct stages of the Terceira Rift reflecting its northwards shift with time (Krause and Watkins, 1970; Vogt and Jung, 2004). Recent earthquake orientations also imply that some of this extension is still active causing numerous and

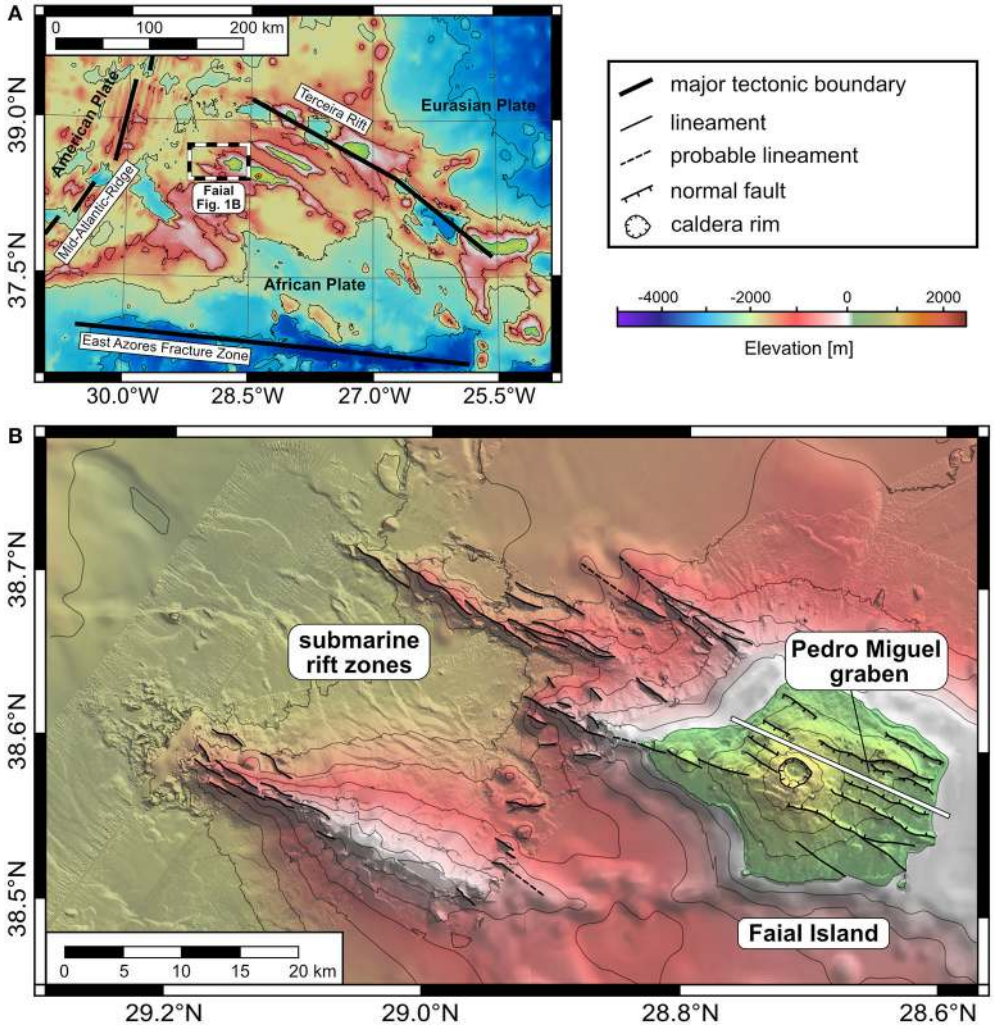

FIGURE 1 | Bathymetric maps and digital elevation models (DEM) of **(A)** the eastern Azores Plateau with major tectonic boundaries (contours are 1000 m elevation) and; **(B)** Faial Island with western adjoining submarine rift zones and major structural features (contours are 250 m elevation). Lineaments and faults on the island modified from Hildenbrand et al. (2012); Tempera et al. (2013); and Trippanera et al. (2014). Thick white line marks the position of the Pedro Miguel graben axis (Trippanera et al., 2014).

destructive earthquakes (e.g., in 1998; Matias et al., 2007), i.e., extension is still taking place in the vicinity of Faial (see also Fontiela et al., 2018).

The Azores Plateau as a whole likely formed from a melting anomaly in the mantle, either due to a small thermal plume head (Schilling, 1975; White et al., 1976; Cannat et al., 1999) or to an anomalous volatile-enriched mantle (Schilling et al., 1980; Bonatti, 1990; Beier et al., 2012; O'Neill and Sigloch, 2018). Noble gas isotopes and melting models suggest that a deep mantle plume may be located beneath Terceira (Moreira et al., 1999, 2018; Bourdon et al., 2005).

Faial Island is located on a subparallel lineament some 50 km SW of the recently active Terceira Rift. Structural features on the island, e.g., the Pedro Miguel graben (Trippanera et al., 2014; Pimentel et al., 2015) and the rift zones show that structures and lineaments on Faial are influenced by the general WNW-ESE striking extensional stress regime prevailing in the eastern Azores Plateau (**Figure 1**), perpendicular to the extensional movement of the African and Eurasian plates (Luis et al., 1998; Weiß et al., 2015a). The subparallel lineaments have previously been interpreted to be extinct rift axes related to the movement of the recently active Terceira Rift. Rift-related structural features on Faial imply that rifting has played a role in the past (Luis et al., 1994; Miranda et al., 1998; Gente et al., 2003) and recent observations of earthquake epicenters suggest that tectonic movements still occur (Fernandes et al., 2002; Dias et al., 2007; Matias et al., 2007; Marques et al., 2013). The extension combined with volcanic activity during the past 1 Ma (Madeira et al., 1995; Hildenbrand et al., 2012; Beier et al., 2015) and the most recent Capelinhos eruption in 1957–1958 provides an opportunity to investigate the interaction between magmatic and tectonic processes in time and space.

Faial can be divided into several volcanic units (Chovelon, 1982; Madeira, 1998; Pacheco, 2001) similar to other volcanic

islands in the Azores. The island is dominated by a central volcano with a caldera. Several adjoining rift zones extend in a north-westerly direction from the Caldeira Volcano into a submarine basin forming the submarine volcanic ridges (**Figure 1**). Similar features are observed along the western flanks of São Miguel (Weiß et al., 2015b). The oldest exposed lavas on the island belong to the Ribeirinha Volcano and were dated at 850–800 ka in the southern part and at 400–350 ka in the north of the volcano. (Hildenbrand et al., 2012; **Figure 2**). Although the younger ages for the northern part of the Ribeirinha Volcano are not supported by computed magnetisations, the gap in radiometric ages indicates a prolonged hiatus between the south and the north (Hildenbrand et al., 2012). However, based on insular shelf data from Quartau and Mitchell (2013) it can be excluded that the Ribeirinha Volcano consists of two central volcanoes. The system rather represents one central volcano with episodic activity, where the older lavas outcrop in the south and the younger eruptives outcrop in the north. A major part of the island consists of the central Caldeira Volcano with lavas dated between ∼120 and ∼40 ka (Hildenbrand et al., 2012), covering most of the older volcanic units. Further younger explosive volcanism through a central vent at the Caldeira Volcano occurred in the last 16 ka, erupting mostly trachytic pyroclastic material (Pimentel et al., 2015). Several studies (e.g., Madeira, 1998; Pacheco, 2001), have proposed that the volcanic activity at the Caldeira Volcano could be as old as 470 ka, based on a single K-Ar age from Demande et al. (1982). However, as discussed in detail in Hildenbrand et al. (2012), this radiometric age may be abnormally old, due to high amounts of pyroxene and olivine phenocrysts in the analyzed whole rock sample. Each volcanic eruption is associated with a distinct developing phase of the eastern and central Pedro Miguel graben (Hildenbrand et al., 2012).

Mafic and intermediate volcanism at the Horta Fissure Zone in the south-eastern part of Faial is exclusively younger than 40 ka (Hildenbrand et al., 2012). At the Capelo Fissure Zone in the western part volcanism is probably younger than 10 ka (Madeira et al., 1995; Madeira, 1998; Di Chiara et al., 2014). Historic eruptions at Capelo Fissure Zone occurred in 1672–1673 at Cabeço do Fogo, and in 1957–1958 at Capelinhos forming a complex tuff cone (Cole et al., 2001).

Generally, volcanism on Faial Island is characterized by short periods of volcanic activity, lasting less than 30 ka, with prolonged hiatuses of up to 500 ka between these periods (Hildenbrand et al., 2012). Hildenbrand et al. (2012) suggest that the volcanic pulses were coeval with tectonic movements and the faulting may be caused partly by deflation of shallow magma reservoirs and partly by extension of the lithosphere. Thus, Faial exhibits similar periodic volcanic activity compared to other islands from the eastern Azores Plateau (e.g., São Jorge, Graciosa; Feraud et al., 1980; Hildenbrand et al., 2008; Larrea et al., 2014; Sibrant et al., 2014).

SAMPLING AND METHODS

Bathymetry and Sampling of the Volcanic Structures

The submarine samples from the rift zones and new bathymetric data were obtained during R/V *Meteor* cruises M113 (Hübscher et al., 2016) and M128 (Beier et al., 2017a; see **Figure 2** for sampling localities). The high resolution bathymetric data were obtained using the hull mounted EM122 and EM710 multi-beam systems with signal frequencies of 12 and 70–100 kHz, respectively. In our working area, most rock samples were taken with a TV-guided grab. Samples from Condor rift (previously also referred to as Condor de Terra, Condor seamount, Condor

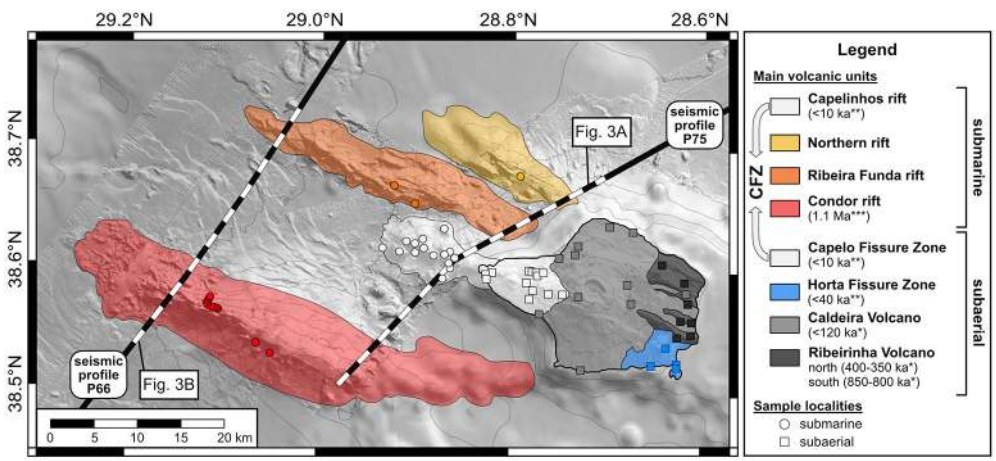

FIGURE 2 | Bathymetric map and DEM of Faial with its neighboring submarine rift zones (same as **Figure 1B**). Superimposed areas marked on the island are different volcanic units with distinct periods of volcanic activity based on K-Ar and radiocarbon ages and models from Hildenbrand et al. (2012) (*) and Madeira et al. (1995) (**). The age for Condor rift is based on Ar-Ar dating from Beier et al. (2015) (***). Black lines mark seismic profiles P66 an P75 from cruise M113, highlighted sections are shown in detail in **Figure 3**. Symbols mark the locations of lava samples, circles refer to submarine and squares to subaerial samples, respectively. The colors are the same as used in the following diagrams and refer to different volcanic units and their respective ages. (CFZ, Central Fissure Zone; comprising the submarine Capelinhos rift and the subaerial Capelo Fissure Zone).

bank, or Condor ridge in the literature, hereafter simply referred to as Condor rift for clarity), taken via Remotely Operated Vehicle (ROV MARUM Quest 4000), were obtained stratigraphically along a vertical profile and along the NW-SE oriented axis. The island of Faial was sampled during several field trips between 2001 and 2003. Samples from cruises Pos232, Pos286 with R/V *Poseidon* and the subaerial samples are the same used in Beier et al. (2012) and Beier et al. (2015).

The subaerial samples from Faial are divided into different volcanic units based on ^{14}C ages and models from Madeira et al. (1995) and K-Ar ages and models from Hildenbrand et al. (2012) according to the sampling localities (**Figure 2**). In this work, we treat the young volcanism at Capelo Fissure Zone and submarine lavas from Capelinhos rift as one geological unit, summarized as the Central Fissure Zone in agreement with a strong structural connection between the subaerial and submarine parts (**Figure 1**, Quartau et al., 2012). Samples from other submarine rift zones are treated as distinct volcanic units for the purpose of our work (**Figure 2**).

Geophysical Methods

The seismic data for this work were obtained during cruise M113 (Hübscher et al., 2016). Seismic signals were generated using an array of three GI-Guns and one Mini-Gun in a water depth of about 2.5 m. The streamer used was a digital 144-channel streamer of 600 m active length. Data processing included frequency filtering (15–350 Hz), gain, velocity analysis (every 50 CMPs), NMO-correction, coherency filtering, stacking, time-migration, bandpass, white noise removal, dip filtering, fx-deconvolution. For a detailed overview of the method see Hübscher and Gohl (2014).

Geochemical Methods

The major element analysis for whole rocks from cruises M113 and M128 were carried out using a Spectro XEPOS He—XRF spectrometer at the GeoZentrum Nordbayern, Friedrich-Alexander Universität Erlangen-Nürnberg using methods described in Woelki et al. (2018). Exactly 1.000 g of dried sample powder was mixed with 4.83 g of lithium tetraborate and 230 mg of di-iodpentoxide, fused to homogenous glass beads using an OXIFLUX burner. The loss on ignition was calculated by the difference between the weighted sample powders to 1 ± 0.0015 g and the same sample powders after 12 h at 1050°C. Using fused glass beads precision and accuracy are better than 0.8% (2σ) and 1% (2σ), respectively, based on repeated measurements of the international rock standard BE-N, BR, and BHVO-1.

The major element analyses of glasses were performed on a JEOL JXA-8200 Superprobe at the GeoZentrum Nordbayern, Universität Erlangen-Nürnberg using methods and standards described in Beier et al. (2017b). An acceleration voltage of 15 kV, a beam current of 15 nA, and a defocused beam (10 μm) were used. Counting times were set to 20 s for peaks and 10 s for backgrounds. Natural volcanic glass standards (basaltic glass standard VG-A99 and rhyolitic glass standard VG-568), together with mineral standards scapolite R-6600 (Smithsonian Institution), apatite, chalcopyrite, fluorite, and rhodonite (P and H Developments) were used for calibration. Glass standards VG-2, VG-A99, and VG-568 were analyzed periodically as unknowns in order to monitor the accuracy of the microprobe result (Brandl et al., 2012).

Trace element analyses for some samples were performed on an Agilent 7500c/s Quadrupole Inductively Coupled Plasma Mass Spectrometer (ICP-MS) at the Institut für Geowissenschaften, Universität zu Kiel. The samples were prepared as described in Beier et al. (2008) and Beier et al. (2012) with a standard deviation of the precision and accuracy of <5% (2σ) and <8% (2σ), respectively, based on repeated standard measurements. Further trace element analyses for submarine and selected subaerial samples from Faial were carried out using a Thermo Fisher Scientific X-Series 2 Quadrupole Inductively Coupled Plasma Mass Spectrometer (ICP-MS) connected to an Aridus 2 membrane desolvating sample introduction system at the GeoZentrum Nordbayern, Friedrich-Alexander Universität Erlangen-Nürnberg. For the dissolution of sample powder and rock standards (BHVO-2) we used the method as described in detail in Freund et al. (2013) following standard techniques using a 3:1 mixture of HF and HNO_3. The dissolved sample solution is diluted accordingly in order to get a dilution factor of about 4000. We use an internal standard containing elements not present in the sample solutions in order to correct the data for machine drifts during the duration of the measurements. Precision and accuracy are better than 1.1% (2σ) and 1.1% (2σ), respectively, based on repeated measurements of the international rock standard BHVO-2.

New Sr-Nd-Pb isotope data from submarine and subaerial samples from Faial were analyzed at the GeoZentrum Nordbayern, Friedrich-Alexander Universität Erlangen-Nürnberg. For Sr-Nd-Pb isotopes ∼150–200 mg dried sample powder were leached in hot 6M HCl for at least 2 h then dissolved (for Sr-Nd-Pb) and separated in ion-exchange columns (for Sr-Nd) using the method described in Haase et al. (2017). Strontium and Nd isotopes were analyzed using a Thermo-Fischer Triton thermal ionization multicollector mass spectrometer in static mode. Strontium isotope measurements were corrected for mass fractionation using $^{88}Sr/^{86}Sr = 0.1194$, and mass 85 monitored to correct for possible contribution of ^{87}Rb to mass 87. Neodymium isotope data were corrected for mass fractionation using a $^{146}Nd/^{144}Nd$ ratio of 0.7219. Samarium interference on masses 144, 148, 150 were corrected for by measuring ^{147}Sm, although the correction was negligible for all samples presented here. During the analysis, SRM987 standard yielded $^{87}Sr/^{86}Sr = 0.710256 \pm 0.000005$, and the Erlangen Nd standard gave $^{143}Nd/^{144}Nd = 0.511543 \pm 0.000003$ (corresponding to a value of 0.511850 for the La Jolla Nd isotope standard). The data were not normalized to the measured standards.

For the digestions and Pb column chemistry only double-distilled acids were used with dropper bottles to keep the blanks as low as possible. For the separation of Pb the dissolved samples were loaded on 100 μl Sr-Spec resin columns and washed with 1M HCl. The Pb was collected using 6M HCl. Lead isotope measurements were carried out on a Thermo-Fisher Neptune MC-ICP-MS using a $^{207}Pb/^{204}Pb$ double spike to correct

for instrumental mass fractionation. The double spike, with a $^{207}Pb/^{204}Pb$ ratio of 0.8135, was calibrated against a solution of the NBS982 equal atom Pb standard. Samples were diluted with 2% HNO_3 to a concentration of ∼20 ppb, and an aliquot of this solution spiked in order to obtain a $^{208}Pb/^{204}Pb$ ratio of about 1. Spiked and unspiked sample solutions were introduced into the plasma via a Cetac Aridus desolvating nebuliser and measured in static mode. Interference of ^{204}Hg on mass 204 was corrected by monitoring ^{202}Hg. An exponential mass fractionation correction was applied offline using the iterative method of Compston and Oversby (1969), the correction was typically 4.5 permil per amu. Twenty measurements of the NBS981 Pb isotope standard (measured as an unknown) over the course of this study gave $^{206}Pb/^{204}Pb$, $^{207}Pb/^{204}Pb$, $^{208}Pb/^{204}Pb$ ratios of 16.9410 ± 0.0020, 15.4993 ± 0.0019, and 36.7244 ± 0.0046 respectively. The Pb blanks are generally below 30 pg. The results for all samples can be found in Supplementary Tables 1 and 2.

RESULTS

Bathymetry

Our bathymetric data west of Faial Island display four WNW-ESE oriented volcanic ridges rising up to 1700 m above the surrounding seafloor (**Figure 1**). These ridges are structurally connected to the island with their south-eastern ends directly joining the western and south-western coast of Faial. Their elevation relative to the sea level decreases with increasing distance from the island. The central Capelinhos rift forms the western submarine extension of the subaerial Capelo Fissure Zone, where the most recent subaerial volcanic activity occurred. South and north of the Capelinhos rift, three rift zones can be distinguished. The Condor rift is located south of Capelinhos rift, the Ribeira Funda, and Northern rifts are located north of the Capelinhos rift (**Figure 2**). Amongst the rift zones north of Capelinhos, the southern rift (Ribeira Funda rift) is along the continuation of a large WNW-ESE subaerial normal fault near the village Ribeira Funda (NW sector of Faial) and the axis of the Pedro Miguel graben (Trippanera et al., 2014) and the northernmost rift zone is situated along the continuation of the northern coast of Faial (Northern rift; **Figure 2**). The length of these submarine rift zones varies between ∼8 km (Capelinhos rift) and ∼50 km (Condor rift), compared to ∼27 km for the SE-NW extent of the island of Faial. Apparently, much of the volcanic activity related to the vicinity of Faial formed only submarine volcanic ridges that did not reach subaerial levels. The WNW-ESE along-rift orientation of the submarine volcanic ridges (∼300°) is similar to the general orientation of faults related to the formation of the Pedro Miguel graben, the alignment and elongation of vents and the orientation of the majority of dikes on the island (Trippanera et al., 2014) and at Condor rift (Tempera et al., 2013). The morphology of the rift zones is dominated by isolated cones or groups of elongated cones and several kilometer-long ridges. In contrast to the Capelinhos rift, the Ribeira Funda, and Northern rifts show evidence for normal faulting in addition to structures related to volcanic activity. Similar features are observed on the island, where the flanks of the Caldeira Volcano and, in particular, the Ribeirinha Volcano are affected by normal faulting, whereas the morphology at the Horta and Capelo Fissure Zones is dominated by dikes and alignments of cones (Trippanera et al., 2014). On a smaller scale the orientation of lineaments within the rift zones does not entirely correspond to their general WNW-ESE orientation. Whereas most rift zones display almost exclusively subparallel oriented lineaments and elongation of cones, several elongated cones along the Capelinhos rift display orientations trending more SW and NW than the dominating orientation of lineaments, forming a fan-shaped system of lineaments (**Figure 1**).

Age Constraints

For the purpose of our work we use both absolute, radiometric, and relative ages from direct observations during ROV dives, geodynamic modeling and seismic profiles. Absolute, radiometric K-Ar and ^{14}C ages from Faial were published in Feraud et al. (1980), Hildenbrand et al. (2012), and Madeira et al. (1995), respectively. They range from 0.848 to 0.03 Ma and 10.25 to 0.32 ka with maximum errors of 0.012 Ma and 1.77 ka, respectively. Last eruptions on the Capelo Fissure Zone occurred in 1672–1673 and recently in 1957–1958 (Capelinhos eruption; Cole et al., 2001). The Capelinhos eruption initially started ∼1.2 km from the old coastline along the Capelinhos rift and rapidly migrated toward the island. The largest uncertainty in the ages used here lies in the submarine samples. Condor rift has been sampled by dredging during R/V *Poseidon* cruise POS 286. A single Ar-Ar age of a submarine lava displays 1.10 ± 0.80 Ma presented in Beier et al. (2015). We note however, that these are minimum ages. Dredging during POS 286 was performed at water depths from 356 to 470 m below sea level, while the ROV profiles during R/V *Meteor* cruise M128 range from 588 to 918 m below sea level. Hence, we treat the age by Beier et al. (2015) as minimum age. We also note that the Ar-Ar age determination on variably altered (Beier et al., 2015, 2017a) mafic submarine volcanic rocks may be challenging. However, geodynamic estimates (Cannat et al., 1999; Gente et al., 2003; Miranda et al., 2018) reveal that much of the igneous basement of Princessa Alice bank, to which Condor's basement may belong, formed at 8–10 Ma. Thus, within the uncertainties of the current ages, we treat Condor rift as the oldest exposed unit in the vicinity of Faial considering that older igneous strata may still be exposed at greater depth but covered by younger lavas. Older ages of formation of Condor rift would significantly strengthen our model presented below.

Seismic Profiles

Relative ages of the different submarine volcanic rift zones west of Faial can be obtained from two seismic profiles each with a length of ∼30 km (**Figure 3**). The two profiles are both SW-NE oriented, perpendicular to the orientation of the rift zones. Profile P75 is located proximal and profile P66 distal relative to Faial (**Figure 2**). P75 comprises all rift zones west of Faial, whereas P66 comprises only the Condor and Ribeira Funda rifts, because these two ridges extend further westwards than the Capelinhos and Northern rifts. In seismic profile P75 all rift zones are significantly elevated against the surrounding seafloor

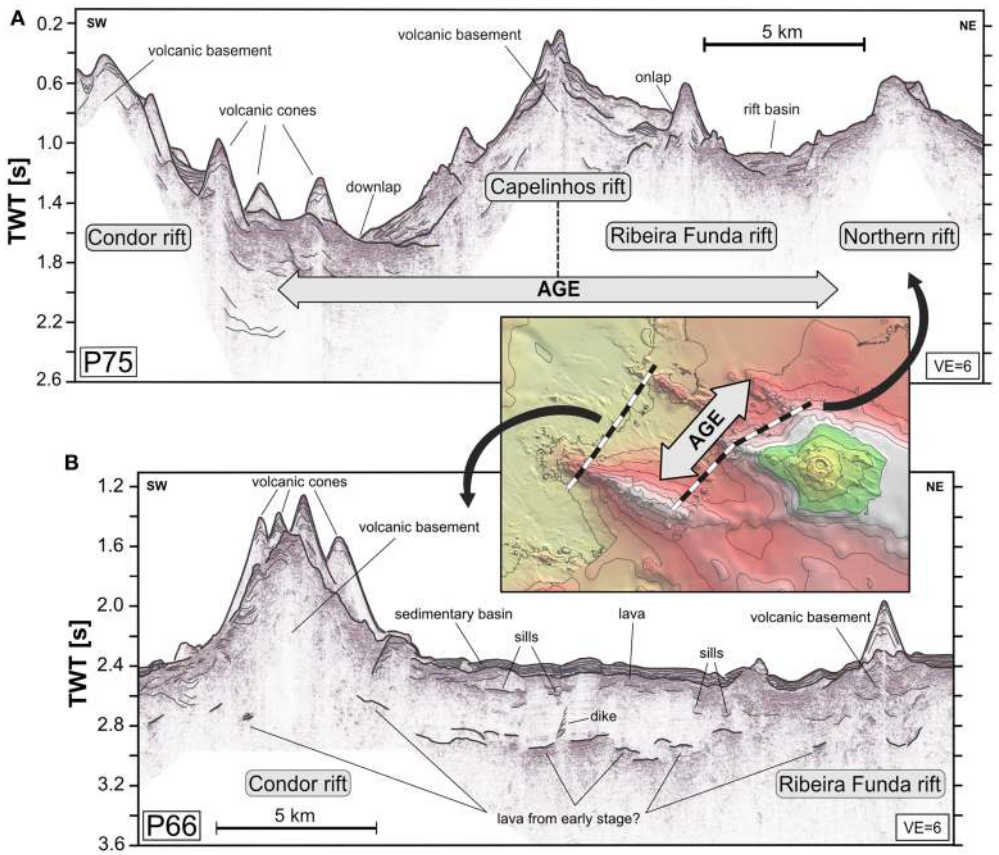

FIGURE 3 | Interpreted SW-NE seismic profiles across the rift zones with **(A)** proximal, and **(B)** distal relative to Faial. Inset map highlights the relative ages derived from seismic imagery, lines mark seismic profiles. Main seismic reflectors are marked with thick black lines. Note that the ages of the rift zones in **(B)** are increasing from Capelinhos rift toward Condor (SW) and Ribeira Funda rifts (NE) as illustrated by the double arrow in **(A)** and the inset map.

(**Figure 3**). The strong reflecting acoustic basement represents the volcanic basement of each rift zone overlain by several less strong reflecting cones. Weak reflecting horizons together with stratified basin fills are associated with marine sediments and debris flows extending from the volcanic bodies toward north-east and south-west (**Figure 3**). Onlap and downlap structures of such debris flows from the Capelinhos rift onto the volcanic basement and debris flows from Condor and Ribeira Funda rifts imply that the Capelinhos rift is younger than the rifts to the north and south. Symmetric and planar layered sediment-filled basins between the Ribeira Funda and Northern rifts suggest that they formed synchronously. The relative age relation between Condor and Ribeira Funda rifts given in profile P66 is less precise compared to the age constraints inferred from P75, because the distance between the rift zones is larger. However, the strong seismic reflection of the volcanic basement of Condor rift is comparable to that observed at Ribeira Funda rift, which may indicate a contemporaneous formation.

Geochemistry and Isotopes

The most abundant rock types from Faial Island and the adjoining rift zones are alkali basalts to trachybasalts, except for some lavas from Condor rift that are classified as tholeiites based on the Total Alkali vs. SiO_2 (TAS) classification of Le Maitre et al. (1989) (Supplementary Figure 1).

Lavas from Faial and associated submarine rift zones from this work range from mafic to evolved rocks covering a MgO content from ∼9 to 1 wt. % (**Figure 4**). Subaerial lavas from the Caldeira and Ribeirinha Volcanoes, ranging from ∼6 to 1 wt. % MgO, equivalent to SiO_2 contents between 45 and 65 wt. %, are generally more evolved than most submarine lavas. Many of the intermediate lavas from the Caldeira Volcano have SiO_2 contents ranging from 53 to 57 wt. %, contrasting observations from other large volcanoes in the Azores, e.g., Santa Barbara Volcano on Terceira (Daly et al., 2012) and the central volcano on Graciosa (Larrea et al., 2018). A larger volume of highly evolved (trachytic) pyroclastic rocks (up to ∼64 wt. % SiO_2 equivalent to MgO contents <1 wt. %) derive from explosive eruptions through a central vent from the Caldeira Volcano. They mainly erupted within the last 16 ka, in part associated with the formation of the caldera (Pimentel et al., 2015). For the purpose of this work, we focus on rock samples covering a range from mafic to intermediate composition (basaltic to trachy-andesitic) to disentangle deep magmatic processes and their interactions with

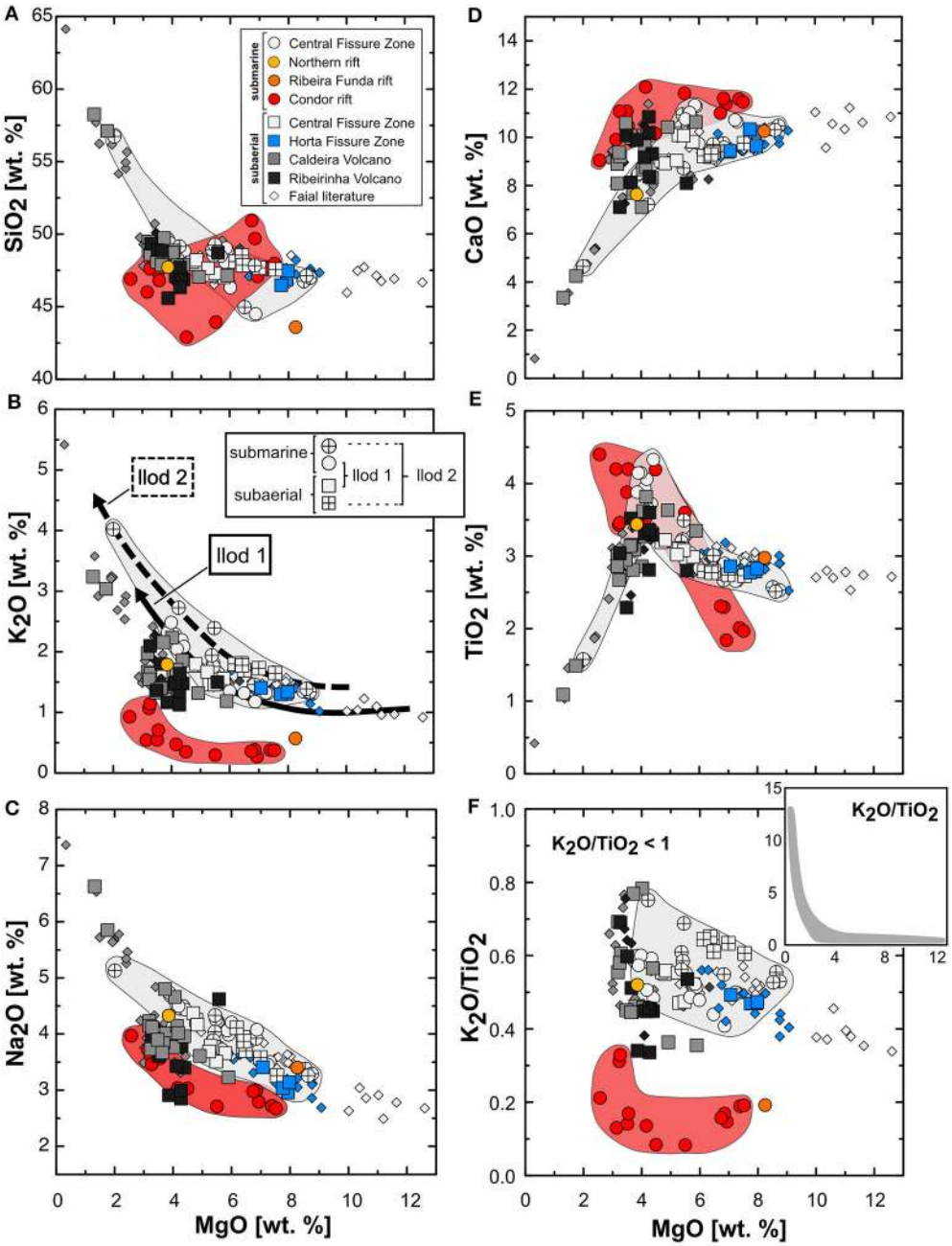

FIGURE 4 | (A-E) Major element contents and **(F)** K_2O/TiO_2 ratios vs. MgO [wt. %]. Symbols are the same as in **Figure 2**. Red and white areas highlight our samples from Condor rift and the Central Fissure Zone, respectively. Two liquid lines of descent with lower (Ilod 1) and higher (Ilod 2) K_2O contents are distinguished [**(B)**, see also **Figure 6**]. Arrows in **(B)** schematically highlight Ilod1 (solid line) and Ilod2 (dashed line). Diamonds are subaerial samples from Zanon et al. (2013) and Hildenbrand et al. (2014). The colors are the same as used for our samples and refer to the respective volcanic units distinguished in **Figure 2**. Inset in **(F)** highlights the range in K_2O/TiO_2 for all Faial lavas. Note that published samples largely overlap those from this study.

tectonic stresses. Thus, we exclude literature data dealing with the silicic (trachytic) eruptions from the Caldeira Volcano <16 ka, i.e., those from Pimentel et al. (2015), because they may rather reflect shallow magmatic processes.

The submarine lavas from the Central Fissure Zone are more evolved than their subaerial equivalents and cover almost the entire range in MgO for lavas from Faial from ∼9 to 2 wt. %, compared to ∼8 to 5 wt. % for the subaerial Central Fissure Zone lavas. The Na_2O, K_2O, and TiO_2 contents at a given MgO content from the Central Fissure Zone are significantly higher compared to both subaerial lavas from the Caldeira and Ribeirinha Volcanoes and submarine lavas from Condor and

Ribeira Funda rifts, however, they are also more variable. At a MgO content of 7 wt. % lavas from the Central Fissure Zone range from 1.2 to 1.7 wt. % K_2O and 3.4 to 4.1 wt. % Na_2O, compared to 0.3 to 0.4 wt. % and 2.8 to 3.0 wt. %, respectively, for lavas from Condor rift (**Figure 4**). Lavas from the Caldeira and Ribeirinha Volcanoes overlap in their K_2O contents. The Na_2O contents of lavas from the Ribeirinha Volcano are lower than those from the Caldeira Volcano ranging from 2.9 to 3.8 wt. % Na_2O compared to 3.8 to 4.7 wt. % Na_2O, respectively. Instead, lavas from Ribeirinha Volcano resemble those from Condor rift.

The incompatible element compositions of lavas from Faial and the rift zones display distinct signatures for the different volcanic units. Lavas from the Central and Horta Fissure Zones have higher La/Yb and Ba/Nb and lower Sm/Nd ratios compared to all other submarine rift zones, except for a single sample (IGSN: IEAZO1169) from the Northern rift (**Figure 5**). An additional Rare-Earth Element diagram is provided in the supplemental material (Supplementary Figure 2). On a larger scale lavas from the Central and Horta Fissure Zones are very similar in their compositions, however on a smaller scale they show subtle differences (Zanon et al., 2013) with lavas from the Central Fissure Zone being slightly more enriched in some incompatible trace element ratios. We use incompatible ratios for lavas between 3 and 5 wt. % MgO, because lavas from the Caldeira and Ribeirinha Volcanoes are mostly covering a comparable range in fractionation indices. We have tested for the influence of fractionation and conclude that most trace element ratios used here are only influenced by fractional crystallization at less than 3 wt. % MgO (**Figure 4**). Subaerial lavas from the Caldeira and Ribeirinha Volcanoes overlap and both lie between those lavas from Condor rift and the Central Fissure Zone with the notable exception of La/Yb ratios. Lavas from the Ribeirinha Volcano have La/Yb of 10 to 13 significantly lower than those from the Caldeira Volcano, ranging from 13 to 21, overlapping with lavas from the Central Fissure Zone (**Figure 5**).

The subaerial and submarine lavas from Faial also display distinct isotope signatures. The overall range is between 0.70343 and 0.70413 for $^{87}Sr/^{86}Sr$ and 0.51303 and 0.51283 for $^{143}Nd/^{144}Nd$, which is within the array of North Atlantic MORB from Dosso et al. (1999) (ranging from 0.70252 to 0.70414 for $^{87}Sr/^{86}Sr$ and 0.51267 to 0.51325 for $^{143}Nd/^{144}Nd$) but shifted toward higher $^{87}Sr/^{86}Sr$ ratios (**Figure 7**). The only exception

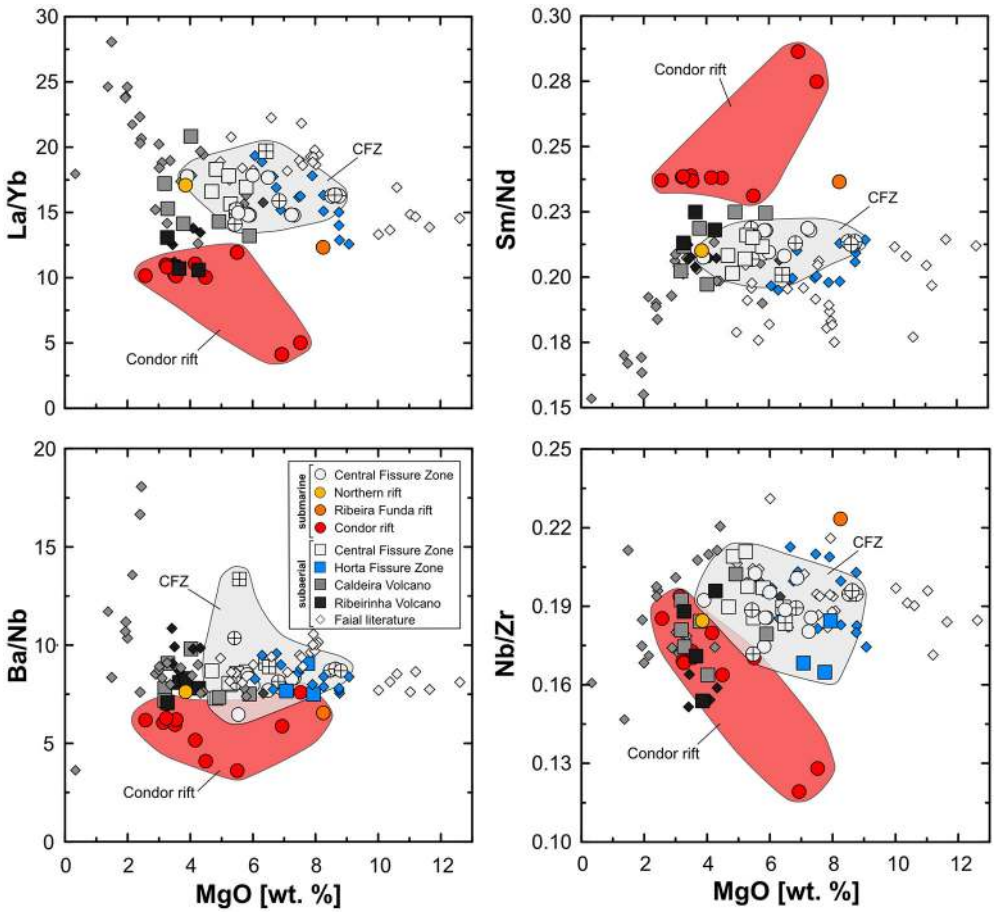

FIGURE 5 | Incompatible trace element variations of submarine and subaerial lavas from Faial. Data sources are the same as in **Figure 4**. (CFZ = Central Fissure Zone).

are the two lowermost samples from the stratigraphic profile at Condor rift (IGSN: IEAZO1135, IEAZO1136) which have notably lower $^{143}Nd/^{144}Nd$ of 0.51274 and 0.51285 compared to other lavas from this section and most other subaerial and submarine lavas. Other samples from Condor and Ribeira Funda rifts display the highest Nd and lowest Sr isotopes, whereas lavas from the Central Fissure Zone have the lowest $^{143}Nd/^{144}Nd$ and highest $^{87}Sr/^{86}Sr$ ratios, except for one sample from the Caldeira Volcano (IGSN: IEAZO0028) which has an elevated Sr isotope composition. Lavas from the Caldeira Volcano cover a large range in Sr-Nd isotope space overlapping with those from the Central Fissure Zone. Lavas from the Ribeirinha Volcano have homogenous Sr-Nd isotope compositions with slightly higher $^{143}Nd/^{144}Nd$ ratios compared to lavas from the Central Fissure Zone and the Caldeira Volcano. The overall range in Pb isotopes for Faial lavas is between 19.187 and 19.623 for $^{206}Pb/^{204}Pb$, 15.540 and 15.652 for $^{207}Pb/^{204}Pb$ and 38.671 and 39.393 for $^{208}Pb/^{204}Pb$. Lavas with the highest $^{87}Sr/^{86}Sr$ and lowest $^{143}Nd/^{144}Nd$ also have the lowest $^{206}Pb/^{204}Pb$ (**Figure 7**). Lavas from Faial lie on a linear array toward more radiogenic $^{207}Pb/^{204}Pb$ and $^{208}Pb/^{204}Pb$ at a given $^{206}Pb/^{204}Pb$ for lavas from the Central Fissure Zone and the Caldeira Volcano compared to lavas from Ribeirinha Volcano and Condor rift (**Figure 7**). Our Sr-Nd-Pb isotope data are in good agreement with those published previously by Hildenbrand et al. (2014) from respective volcanic units. Generally, lavas from Faial have slightly lower $^{206}Pb/^{204}Pb$ at similar $^{207}Pb/^{204}Pb$ and $^{208}Pb/^{204}Pb$ ratios compared to other islands from the Central Azores Plateau, i.e., Pico and São Jorge ($^{206}Pb/^{204}Pb = 19.347$ to 20.092; $^{207}Pb/^{204}Pb = 15.540$ to 15.650; $^{208}Pb/^{204}Pb = 38.744$ to 39.510; **Figure 7**). In Sr-Nd space, however, lavas from Faial cover a larger range in $^{87}Sr/^{86}Sr$ and a slightly elevated $^{143}Nd/^{144}Nd$ compared to samples from both Pico and São Jorge (ranging from 0.70338 to 0.70406 for $^{87}Sr/^{86}Sr$ and 0.51281 to 0.51300 for $^{143}Nd/^{144}Nd$; **Figure 7**).

In summary, lavas from different volcanic units on Faial and submarine rift zones generally have distinct major and trace element and Sr-Nd-Pb isotope signatures. The two most extreme compositions are observed in lavas from the Central Fissure Zone with the highest K_2O contents (at a given MgO content) and most radiogenic Sr and Pb isotope ratios compared to other subaerial and submarine units. Lavas from Condor rift display the lowest K_2O contents and least radiogenic Sr-Pb isotope ratios. Lavas from other volcanic units show major element, trace element and isotope pattern between these two groups. Comprehensive selected major and trace elements, and Sr-Nd-Pb isotopes from all volcanic units on Faial and submarine volcanic rift zones are provided in **Table 1**.

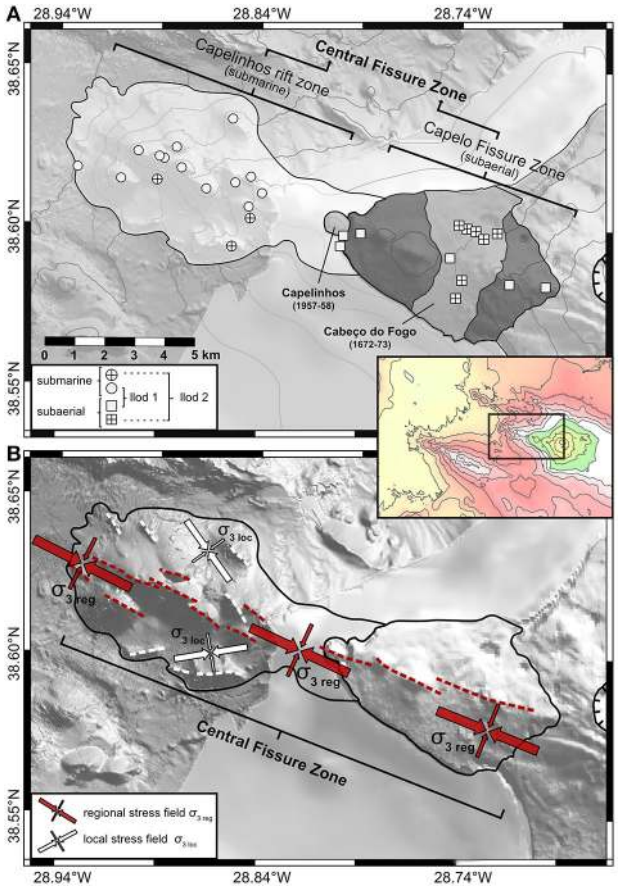

FIGURE 6 | Bathymetric map and DEM of the Central Fissure Zone comprising of a submarine part (Capelinhos rift) and a subaerial part (Capelo Fissure Zone). In **(A)** different smaller volcanic units are shown and refer to historic eruptions along the Central Fissure Zone. Numbers in brackets are year of eruption (A.D.). Symbols are the same as in **Figure 4** and refer to two liquid lines of descent with lower (llod 1) and higher (llod 2) K_2O contents. **(B)** Schematic model of the local and regional stress fields during the formation of the Central Fissure Zone. Red dashed lines and arrows display the orientation of lineaments reflecting the regional stress field (σ_{3reg} perpendicular to the WNW-ESE lineaments); white dashed lines and arrows display the orientation of the local stress field (σ_{3loc} perpendicular to NW-SE and WSW-ENE lineaments). Inset map for orientation.

DISCUSSION

The Formation of the Volcanic Rift Zones

The morphological, structural and geochemical features on Faial have been subject of several detailed studies in the last two decades (Madeira, 1998; Pacheco, 2001; Matias et al., 2007; Hildenbrand et al., 2012; Zanon and Frezzotti, 2013; Zanon et al., 2013; Di Chiara et al., 2014; Marques et al., 2014; Trippanera et al., 2014; Pimentel et al., 2015). Lithospheric extension is a major feature influencing both the morphology and structure of volcanic units forming the island. Bathymetric data from the seafloor west of Faial reveal that much of the volcanic activity is situated below sea level along WNW-ESE oriented rift zones, covering roughly the same areal extent compared to the subaerial volcanic units forming the island (**Figure 1**). In contrast to the central volcanic edifices, i.e., the Ribeirinha Volcano and Caldeira Volcano, which comprise a major volume of the island, the submarine volcanism occurs along narrow rift zones extending from the island over tens of kilometers into the basin. The submarine volcanism is structurally comparable to that occurring subaerially at the Capelo and Horta Fissure Zones, consisting mostly of fissure eruptions, isolated cones and alignments of

TABLE 1 | Comprehensive selected major and trace elements, and Sr-Nd-Pb isotopes from Faial Island and submarine volcanic rift zones.

Sample	**AZF-03-11**	**AZF-03-12**	**AZF-03-02**	**AZF-03-17**	**AZF-03-28**
IGSN	IEAZO0011	IEAZO0012	IEAZO0002	IEAZO0017	IEAZO0028
Location	Capelo FZ	Capelo FZ	Caldeira Volc.	Ribeirinha Volc.	Ribeirinha Volc.
Latitude (N)	38.596	38.592	38.519	38.547	38.583
Longitude (W)	28.826	28.827	28.725	28.626	28.614
Elevation (m)	62	8	10	78	155
(wt. %)					
SiO_2	*47.29*	*48.22*	*49.49*	*49.34*	*48.73*
TiO_2	*3.08*	*3.22*	*2.86*	*3.04*	*2.86*
Al_2O_3	*16.87*	*16.97*	*17.87*	*16.72*	*17.61*
FeO^T	*9.70*	*9.90*	*8.93*	*10.60*	*9.69*
MnO	*0.16*	*0.16*	*0.16*	*0.20*	*0.17*
MgO	*5.47*	*4.83*	*3.18*	*3.27*	*4.02*
CaO	*10.07*	*8.92*	*8.09*	*7.10*	*7.10*
Na_2O	*3.51*	*4.17*	*4.23*	*3.95*	*3.77*
K_2O	*1.46*	*1.80*	*1.98*	*2.10*	*2.24*
P_2O_5	*0.56*	*0.64*	*0.70*	*0.61*	*0.73*
SO_3	–	–	–	–	–
Cl	–	–	–	–	–
LOI	*0.060*	–	*0.710*	*1.31*	*1.26*
Total	*99.31*	*99.93*	*99.19*	*99.42*	*99.26*
(ppm)					
Rb	*31.7*	*41.9*	*42.6*	*43.4*	*47.9*
Sr	*747*	*749*	*749*	*565*	*791*
Y	*28.5*	*35.7*	*40.1*	*47.5*	*36.3*
Zr	*251*	*303*	*347*	*380*	*405*
Nb	*46.5*	*63.3*	*66.8*	*71.4*	*66.2*
Cs	*0.306*	*0.284*	*0.268*	*0.085*	*0.211*
Ba	*398*	*462*	*522*	*505*	*650*
La	*37.7*	*44.8*	*48.9*	*46.8*	*66.1*
Ce	*82.2*	*85.5*	*107*	*90.3*	*131*
Pr	*9.99*	*10.2*	*12.8*	*11.0*	*15.7*
Nd	*40.5*	*41.2*	*49.9*	*45.1*	*60.1*
Sm	*8.71*	*8.30*	*10.1*	*9.62*	*11.9*
Eu	*2.75*	*2.64*	*3.06*	*3.06*	*3.50*
Gd	*7.92*	*7.61*	*9.19*	*9.18*	*10.3*
Tb	*1.15*	*1.12*	*1.31*	*1.41*	*1.48*
Dy	*6.42*	*6.02*	*7.10*	*7.85*	*8.04*
Ho	*1.16*	*1.13*	*1.30*	*1.52*	*1.45*
Er	*2.98*	*2.88*	*3.36*	*3.93*	*3.76*
Tm	*0.396*	*0.398*	*0.450*	*0.564*	*0.507*
Yb	*2.49*	*2.45*	*2.84*	*3.57*	*3.17*
Lu	*0.347*	*0.353*	*0.401*	*0.530*	*0.442*
Hf	*6.05*	*5.91*	*7.74*	*7.11*	*9.42*
Ta	*3.02*	*3.11*	*3.52*	*3.35*	*4.18*
Pb	*2.75*	*3.12*	*3.12*	*2.77*	*4.41*
Th	*3.46*	*4.54*	*4.81*	*5.53*	*6.38*
U	*1.06*	*1.34*	*1.58*	*1.03*	*1.61*
$^{87}Sr/^{86}Sr$	*0.703840*	*0.703861*	*0.703888*	*0.703769*	*0.704129*
$^{143}Nd/^{144}Nd$	*0.512881*	*0.512858*	*0.512881*	*0.512916*	*0.512834*
$^{206}Pb/^{204}Pb$	*19.618*	19.567	19.563	19.314	19.437
$^{207}Pb/^{204}Pb$	*15.647*	15.641	15.639	15.553	15.624
$^{208}Pb/^{204}Pb$	*39.331*	39.286	39.238	38.819	39.140

(Continued)

TABLE 1 | Continued

Sample	814TVG-01	820TVG-01	817ROV-01	817ROV-07	817ROV-13
IGSN	IEAZO1131	IEAZO1151	IEAZO1135	IEAZO1141	IEAZO1147
Location	Capelinhos rift	Capelinhos rift	Condor rift	Condor rift	Condor rift
Latitude (N)	38.623	38.618	38.573	38.569	38.566
Longitude (W)	28.909	28.892	29.114	29.116	29.107
Elevation (m)	–663	–427	–918	–734	–588
(wt. %)					
SiO_2	46.32	49.42	46.91	43.94	47.18
TiO_2	2.84	4.15	4.40	3.60	3.52
Al_2O_3	17.94	15.30	18.54	17.56	18.49
FeO^T	9.33	11.07	10.29	10.85	8.63
MnO	0.16	0.20	0.13	0.13	0.12
MgO	6.00	3.90	2.57	5.50	4.16
CaO	9.74	8.50	9.05	11.82	12.08
Na_2O	4.21	4.69	3.97	2.71	3.04
K_2O	1.35	2.37	0.93	0.30	0.48
P_2O_5	0.62	0.97	0.53	0.59	0.32
SO_3	–	0.12	–	–	–
Cl	–	0.10	–	–	–
LOI	0.17	–	1.27	1.51	0.77
Total	99.71	100.76	99.73	99.73	99.75
(ppm)					
Rb	26.4	31.2	5.28	1.57	2.62
Sr	750	771	381	475	459
Y	28.7	31.9	36.6	22.7	27.5
Zr	248	296	218	165	185
Nb	48.5	56.9	40.4	28.1	33.3
Cs	–	–	–	–	–
Ba	386	444	250	101	172
La	36.8	42.0	29.8	21.0	23.3
Ce	70.7	82.9	58.5	42.2	47.6
Pr	8.76	10.3	7.57	5.30	6.16
Nd	36.1	42.6	33.0	22.6	26.7
Sm	7.57	8.84	7.82	5.22	6.35
Eu	2.33	2.71	2.43	1.63	2.05
Gd	6.89	7.98	7.97	5.16	6.29
Tb	0.981	1.14	1.20	0.770	0.936
Dy	5.54	6.43	7.09	4.43	5.43
Ho	0.994	1.15	1.33	0.814	0.995
Er	2.59	2.98	3.58	2.17	2.62
Tm	0.340	0.394	0.485	0.290	0.347
Yb	2.06	2.36	2.93	1.76	2.11
Lu	0.299	0.344	0.439	0.262	0.308
Hf	5.67	6.60	6.15	3.94	4.80
Ta	2.96	3.41	2.59	1.81	2.13
Pb	2.71	3.03	2.75	1.63	1.61
Th	3.37	3.88	2.91	2.09	2.23
U	0.971	1.13	2.92	1.58	1.00
$^{87}Sr/^{86}Sr$	0.703873	0.703812	0.703718	0.703686	0.703775
$^{143}Nd/^{144}Nd$	0.512870	0.512865	0.512737	0.512930	0.512925
$^{206}Pb/^{204}Pb$	19.528	19.468	19.187	19.502	19.439
$^{207}Pb/^{204}Pb$	15.643	15.642	15.624	15.608	15.571
$^{208}Pb/^{204}Pb$	39.272	39.241	38.946	38.924	38.884

Italic data were analyzed and published as described in Beier et al. (2012).

elongated cones, and dikes (Zanon et al., 2013; Trippanera et al., 2014). This is in contrast to eruptions forming the Caldeira Volcano and probably the Ribeirinha Volcano, which are large central volcanoes.

Generally, there are two different directions of lineations influencing the volcanic units on the island. Most structures, including those showing fissural and monogenetic volcanism along the Capelo and Horta Fissure Zones, are oriented

WNW-ESE with extension taking place in a mean 045° direction (Trippanera et al., 2014, **Figures 1**, **6**). Central volcanic edifices, e.g., the Caldeira Volcano, however, additionally show less dominant structures with a NNE-SSW orientation, which may be the result of far-field effects of activity along the MAR (Trippanera et al., 2014) or may be due to local stresses during magma emplacement. The orientation of the submarine rift zones (∼300°), parallel to the dominating WNW-ESE orientation of most lineaments on the island of Faial, indicate that they are also influenced by the general regional tectonic stress field prevailing at Faial (**Figures 1**, **6**). Studies on, e.g., Iceland have shown that melts can be transported along dikes up to tens of kilometers causing fissure eruptions and alignments of monogenetic cones, like the 2014 dike emplacements near Bardarbunga Volcano (Gudmundsson et al., 2014, 2016; Sigmundsson et al., 2014). Dikes are usually oriented rift-parallel and perpendicular to the least principal compressive stress σ_3 and, therefore, reflect the regional stress field (Schwarz et al., 2005). The occurrence and orientation of dikes in a mean 311° ± 15° direction on Faial (Trippanera et al., 2014) corresponds to the orientation of the submarine rift zones. Thus, we suggest that the lateral transport of melts via dikes into the basin is the major process during the formation of the rift zones. The direction of dikes on Faial is indeed slightly rotated against the general direction of lineaments (mean of 298° ± 16°(Trippanera et al., 2014), however, this is rather an effect of shallow en-echelon dyking, comparable to that observed at Desertas Islands in the Madeira archipelago (Klügel et al., 2005b; Trippanera et al., 2014).

Lineaments at the Capelinhos rift, differing from the otherwise consistent WNW-ESE orientation, reflect local rather than regional changes in the stress field. These lineaments are located at the north-eastern and south-western flanks of the Capelinhos rift in ∼265° and ∼320° directions, respectively (**Figure 6**). A recent study by Tibaldi et al. (2014) has shown that eruptions at the flanks of elongated volcanic edifices may result in locally rotated stress fields which are related to gravity forces and controlled by the topography forming a diverging volcanic rift system. We conclude that the fan-like arrangement of lineaments at Capelinhos rift is the result of a combination of dike emplacement at the flanks of existing volcanic edifices, the shallow rotation of σ_3 and, subsequently, a local change in the orientation of lineaments from the predominant WNW-ESE to a more E-W and NW-SE direction (**Figure 6**).

Lavas from the western tip of Faial (Capelo Fissure Zone) have erupted within the last ∼10 ka and represent the youngest volcanic unit on Faial (Madeira et al., 1995; Hildenbrand et al., 2012; Di Chiara et al., 2014). Samples taken along the western adjoining submarine Capelinhos rift using visual sampling techniques during R/V *Meteor* cruise M128 reveal that these are fresh, glassy lavas with scarce biological coatings (Beier et al., 2017a). We conclude that lavas along the entire Capelinhos rift are as young as those erupted subaerially along the Capelo Fissure Zone (<10 ka) forming a single volcanic unit. Lavas taken along the rift zones north and south of Capelinhos rift are strongly altered with biological overgrowths and are covered by carbonate sand and debris. Representative images of rock samples and the ocean seafloor west of Faial are provided in the supplements (Supplementary Figure 3) and in Beier et al. (2017a).

For the submarine rift zones north and south of Capelinhos rift, we combine absolute ages from geochronology with seismic data providing relative age constraints between individual larger units (**Figure 3**). In agreement with Ar-Ar ages and direct observations using visual sampling techniques, the seismic profiles show that the age of the rift zones increases with increasing distance from Capelinhos rift systematically to the south (Condor rift) and north (Ribeira Funda and Northern rifts; **Figure 3**). They are covering an age range from 1.1 Ma until recently, based on Ar-Ar ages from Beier et al. (2015). Hence, we have grouped our samples into subaerial and submarine lavas consistent with their approximate ages (**Figure 2**).

The seismic data allow to constrain the relative ages between the Ribeira Funda and Capelinhos rifts, but it is much more difficult to determine the age of Ribeira Funda rift relative to units on the island or Condor rift. In this case, structural features, however, can be used for a rough estimate of the relative age of the volcanic activity along Ribeira Funda. The Ribeira Funda rift has the same orientation and is located in the extension of the Pedro Miguel graben axis (**Figure 1**), which was active at 400 ka (Hildenbrand et al., 2012). We suggest that this strong structural connection could be explained by a contemporaneous formation. The internal structure of Ribeira Funda rift evidences normal faulting, in contrast to the Central Fissure Zone (**Figure 3**). This implies that Ribeira Funda rift was formed when tectonic activity along the Pedro Miguel graben began and was already formed while the displacement at the graben was still active, with the result that the existing ridge was rifted. Assuming that the orientation of the rift zones mirrors the tectonic stress field, it has not changed significantly during their evolution. Note that the submarine rift zones probably cover the entire age interval of subaerial volcanic activity on Faial (∼1 Ma until recently). This contrasts observations from São Miguel and to some extent Santa Maria, which experienced distinct major stress fields during their formation due to the reconfiguration of the Africa-Eurasia plate boundary (Sibrant et al., 2015, 2016; Ramalho et al., 2017).

Geochemical Relationship Between the Rift Zone Lavas

Models dealing with the formation of volcanic rift zones and dike emplacement suggest a central accumulation zone of melts feeding a central volcano, from which sills and dikes intrude along rift zones depending on the local and regional stress fields (e.g., Gudmundsson, 1995; Garcia et al., 1996; Paquet et al., 2007; Gudmundsson et al., 2014). These models have in common that melts feeding both the central volcanoes and the associated rift zones form from the same shallow crustal reservoir. The magmatic system of Faial consists of both large central volcanoes and distinct, individual rift zones with lavas derived from fissure eruptions and dyking deviating in age on the order of several 100 ka. This allows to test whether melts erupted from different volcanic structures (i.e., central volcanoes or rift zones) systematically deviate in source and composition and to determine what

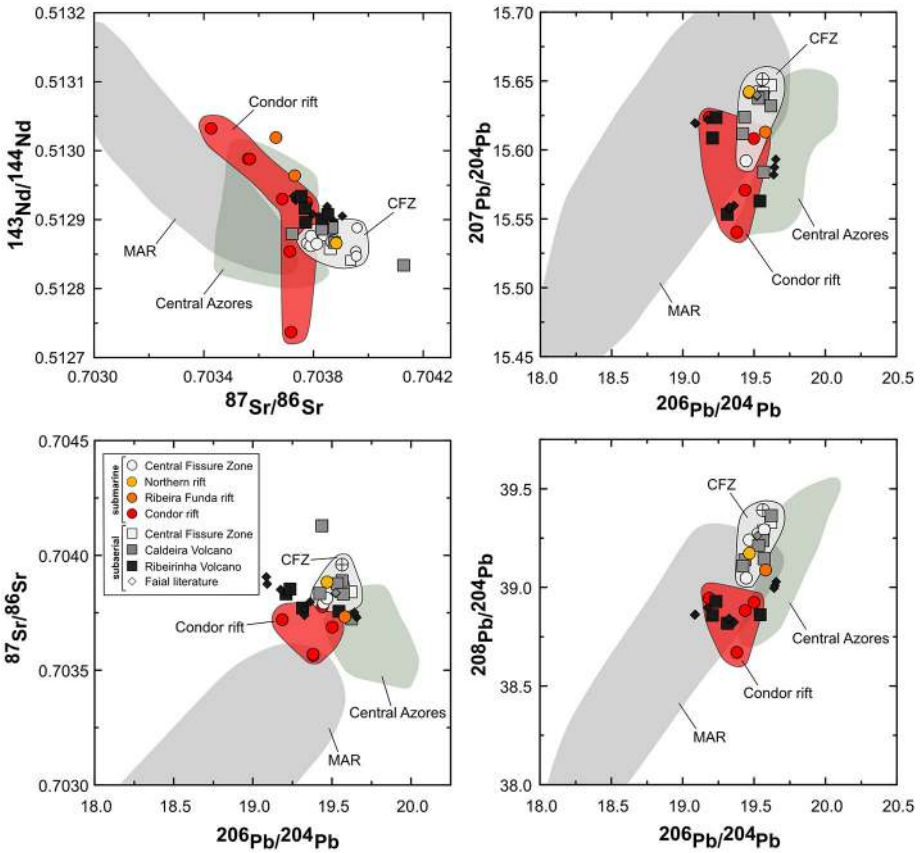

FIGURE 7 | Strontium-Nd-Pb isotope ratios of submarine and subaerial lavas from Faial. Green highlighted areas are samples from the Central Azores Plateau (São Jorge and Pico) from Hildenbrand et al. (2008), Beier et al. (2012), and Hildenbrand et al. (2014). Gray field are samples from the Mid-Atlantic-Ridge (MAR) from Dosso et al. (1999). CFZ, Central Fissure Zone.

the spatial and temporal parameters are that influence the melts.

All lavas from Faial and from the submarine rift zones display evidence for fractional crystallization during magma ascent. Most major elements (CaO, K_2O, Na_2O, FeO^T, and Al_2O_3) are correlated with fractionation indices, e.g., MgO (**Figure 4**) and SiO_2. The most primitive lava from Faial in this work has a MgO content of 8.62 wt. % (IGSN: IEAZO0651) and, thus is significantly more evolved than primitive lavas from the islands along the Terceira Rift with about 10–12.5 wt. % MgO (Beier et al., 2006, 2008). Zanon et al. (2013) showed that some Faial lavas have MgO contents up 12.5 wt. % (**Figure 4**) but their lavas with >10 wt. % MgO are highly porphyritic ankaramites and are thus considered to be the result of accumulation of olivine and clinopyroxene crystals. We conclude that the most primitive submarine and subaerial rocks from Faial have about 9 to 10 wt. % MgO in equilibrium with forsterite contents of Fo_{79} in olivines (Roeder and Emslie, 1970) analyzed in these lavas (Beier et al., 2012). Generally, lavas from the Caldeira and Ribeirinha Volcanoes are more evolved compared to other samples from the island and rift zones (**Figure 4**). We suggest that extensive fractional crystallization is dominant in these large volcanic edifices compared to lavas from the submarine rift zones and subaerial fissure zones. This is in agreement with thermobarometric calculations from Zanon et al. (2013) and Zanon and Frezzotti (2013), which have shown that rocks derived from fissure eruptions at the Capelo and Horta Fissure Zones have not stagnated significantly during their ascent from the mantle, whereas melts at the Caldeira Volcano have undergone polybaric fractional crystallization and stagnation at shallower crustal levels, leading to the formation of trachytes (Pimentel et al., 2015). The variability of most major elements, in particular K_2O, and incompatible trace element ratios, (e.g., La/Yb, Nb/Zr) at a given MgO content (**Figures 4**, **5**) however, cannot be explained by simple fractional crystallization and may rather be related to changes in mantle source composition or degree of partial melting, respectively (see below). We conclude that lavas from different subaerial and submarine units cannot be related to crystallization along a single liquid line of descent but may have experienced similar degrees of fractionation.

We also observe variable major element contents in single volcanic units. Using samples from the Central Fissure Zone as the best sampled unit, some major elements, in particular K_2O, imply that there are two slightly distinct liquid lines of descent

even within a volcanic unit (**Figures 4**, **6**). As a result, we divide the Central Fissure Zone lavas into two groups each representing liquid lines of descent with lower and higher K_2O contents, respectively. Small-scale compositional variations within a single volcanic system are also well-known from other oceanic volcanic systems (e.g., the 1783 Laki eruption; Neave et al., 2013) where multiple lines of evidence contradict the evolution of the erupted magma along a single liquid line of descent. Samples from recent eruptions along the Central Fissure Zone, including those from the 1957–58 Capelinhos eruption, form a lower K_2O liquid line of descent (llod1). Whereas most lavas from the historic 1672–73 Cabeço do Fogo eruption and a few submarine lavas from the Capelinhos rift lie on a liquid line with higher K_2O contents (llod2). Combining our data with those from Zanon et al. (2013), there is no clear correlation with historic eruption centers. Several other eruptions occurred within the last 10 ka along the Central Fissure Zone on a small spatial area which may be the result of overlapping eruptions. More importantly, lavas from both liquid lines of descent occur subaerially and along the entire submarine rift axis (**Figure 6**). We thus conclude that there are several magmatic phases in which melts are efficiently transported laterally within relatively short timescales over several kilometers (>12 km) along the rift zones prior to eruption, probably via sills and dikes.

This implies that melts erupted at length scales of <12 km, i.e., the length of Central Fissure Zone rift, provide information on the geochemical variability within relatively short timescales. Comparison of the northern and southern rift zones relative to submarine and subaerial lavas from Faial may, on the other hand, provide information on the temporal evolution of the melts over <1 Ma during which these rift zones have been active. The high K_2O and Na_2O contents of lavas from the Central Fissure Zone compared to the other lavas from the island and the rift zones (**Figure 4**) indicate that there are several magmatic series erupting along the rift zones and the central volcanoes. The distinct major element compositions not related to fractional crystallization thus may result from systematic changes in either the conditions and/or sources of melting and/or the tectonic regime influencing the magmatic system beneath Faial.

Melting Regime

Source of Melting

Incompatible trace element ratios can be used to distinguish between mantle sources (e.g., Sun and McDonough, 1989; Hofmann, 2003; and references therein). The variable K_2O contents and K_2O/TiO_2 ratios (**Figure 4**) of lavas from Faial combined with variable incompatible trace element ratios, e.g., Nb/Zr, Ba/Nb, Sm/Nd (**Figure 5**) and their Sr-Nd-Pb isotope compositions (**Figure 7**) indicate that subaerial and submarine lavas can indeed be distinguished based on their mantle source signatures. Lavas from Condor and Ribeira Funda rifts have lower Ba/Nb and higher Sm/Nd at a given MgO content and lower $^{87}Sr/^{86}Sr$ and higher $^{143}Nd/^{144}Nd$ isotope ratios, respectively, compared to lavas from the Central Fissure Zone. We suggest that lavas from Condor and Ribeira Funda rifts may have originated from a more depleted mantle source compared to Central Fissure Zone melts. The two stratigraphically lowermost lavas from the Condor section with lower $^{143}Nd/^{144}Nd$ are likely to reflect a more enriched mantle source compared to other lavas from this rift zone. Considering their relative stratigraphic position, we suggest that they are the oldest samples from Condor rift and might reflect a former more enriched mantle source which has progressively changed in composition toward the younger volcanism along this ridge. In agreement, the $^{206}Pb/^{204}Pb$ ratios are lower for lavas from Condor rift compared to those from the Central Fissure Zone. Lavas from Ribeira Funda rift tend to slightly more radiogenic $^{207}Pb/^{204}Pb$ and $^{208}Pb/^{204}Pb$ ratios compared to Condor rift at a given $^{206}Pb/^{204}Pb$ (**Figure 7**). Thus, melts feeding the volcanism on Faial and submarine rift zones originate from a variably heterogeneous mantle similar to that observed in other Azores islands (Hawkesworth et al., 1979; Turner et al., 1997; Widom et al., 1997; Haase and Beier, 2003; Beier et al., 2007, 2008; Elliott et al., 2007; Madureira et al., 2011).

The difference between the Condor rift and the Central Fissure Zone lavas indicates that the mantle source compositions became more radiogenic in Sr and Pb isotope compositions with decreasing age. The mantle source signatures for lavas from the Caldeira and Ribeirinha Volcanoes lie between those from the Central Fissure Zone and Condor and Ribeira Funda rifts, based on their K_2O contents and most incompatible element ratios (**Figures 4**, **5**) at a given MgO content. The Sr-Nd isotope ratios of the Ribeirinha Volcano suggest a slightly more depleted source than those from the Central Fissure Zone, whereas lavas from the Caldeira Volcano overlap those of the young lavas forming the Central Fissure Zone (**Figure 7**). Samples associated with the Ribeirinha Volcano deviate in Pb isotopes toward less radiogenic $^{207}Pb/^{204}Pb$ and $^{208}Pb/^{204}Pb$ ratios compared to the Caldeira Volcano consistent with small variations in major and trace elements. If Faial is treated as a single magmatic system, the trace element and isotope variability between distinct lava suites implies continuous trends in which some lavas form a compositional transition between the two most extreme compositions. We thus suggest that these lavas originate from a comparatively enriched but heterogeneous mantle. Combining these observations with the ages of the distinct lava suites implies that Faial lavas have experienced a progressive enrichment of the mantle source with time (**Figures 7**, **8**, **10**). Thus, as the chemical signatures of the Ribeira Funda rift lavas are comparable to lavas from Condor rift and the Ribeirinha Volcano, we suggest that Ribeira Funda rift is probably older than the Caldeira Volcano (**Figure 10**).

The progressive evolution of the mantle source composition is accompanied by changes in the spatial distribution of the volcanism. Older lavas with a more depleted mantle source composition cover a large spatial area, whereas the youngest and most enriched lavas erupted along a single rift zone, indicating that the composition of melts and their spatial distribution may be linked, the significance of which we will discuss below.

Conditions of Melting

The degree of partial melting can be estimated using moderately incompatible elements, e.g., Na_2O (Klein and Langmuir, 1987; Prytulak and Elliott, 2007) and incompatible trace element

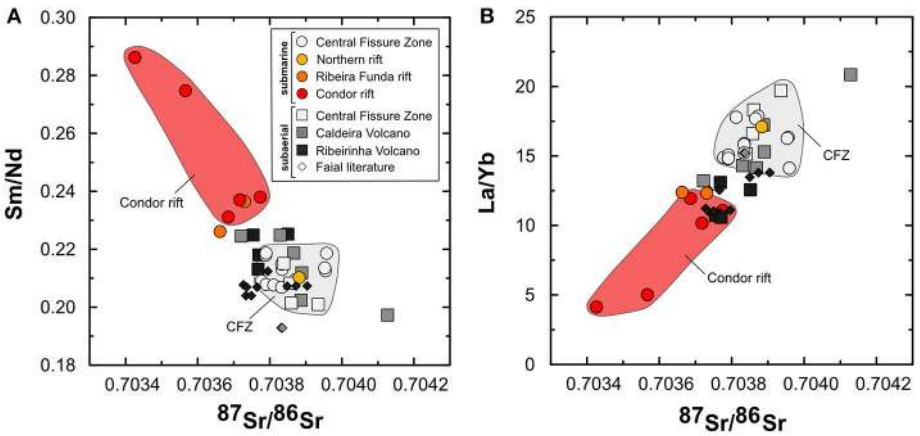

FIGURE 8 | Variations of **(A)** source sensitive trace element ratio Sm/Nd and **(B)** melting sensitive trace element ratios La/Yb vs. $^{87}Sr/^{86}Sr$. Data sources are the same as in **Figure 4**.

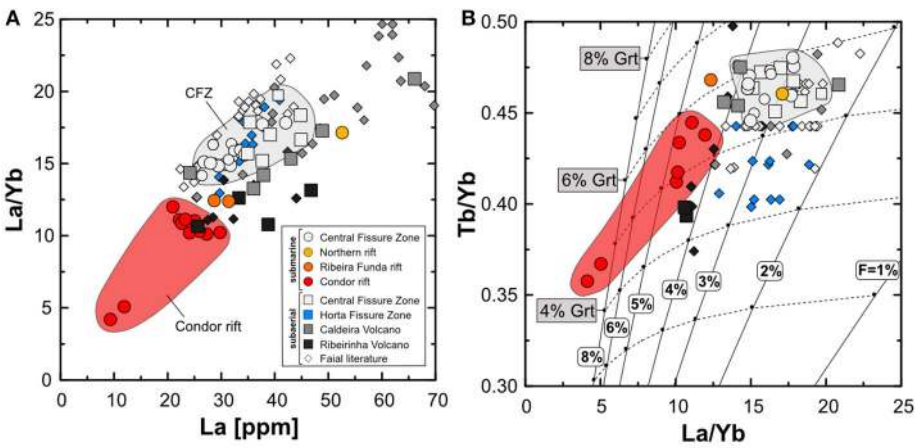

FIGURE 9 | La/Yb vs. **(A)** elemental concentration of La [ppm] and; **(B)** Fractional melting model modified from Bourdon et al. (2005) and Beier et al. (2013) for Faial lavas using a Tb/Yb vs. La/Yb space and a primitive mantle source from Sun and McDonough (1989) comprised of 55% olivine, 25% orthopyroxene and variable ratios of clinopyroxene and garnet as shown by gray boxes and dashed lines, respectively. White boxes and solid lines mark the degree of partial melting. Partition coefficients for olivine, orthopyroxene, and clinopyroxene were taken from those compiled in Halliday et al. (1995) and references therein, Adam and Green (2006) and Villemant et al. (1981), for garnet from Green et al. (2000). The distribution coefficients used for this model can be found in Supplementary Table 3. Data sources are the same as in **Figure 4**.

ratios, e.g., La/Yb. These values represent mean degrees of melting, given that most oceanic basalts probably represent the accumulated products of a continuous melting process that generates instantaneous melts at a range of melt fractions. Two groups can be distinguished based on their distinct La/Yb ratios (**Figure 9**). The consistently higher Na_2O contents and La/Yb ratios from the Central Fissure Zone imply slightly smaller degrees of partial melting compared to most of the surrounding volcanoes and rift zones (**Figures 4**, **5**). Both submarine lavas from Condor and Ribeira Funda rifts and subaerial lavas from the Ribeirinha Volcano indicate higher degrees of partial melting (based on lower La/Yb ratios), relative to lavas from the Central Fissure Zone and the Caldeira Volcano. These groups are similar to those observed with respect to their mantle source compositions, except for Ribeirinha Volcano which has a similar degree of partial melting compared to Condor rift but a more enriched source composition. Incompatible trace elements sensitive to either mantle source signatures (e.g., Sm/Nd) and the degree of partial melting (e.g., La/Yb) correlate with Sr-Nd isotope compositions (**Figure 8**) implying a heterogeneous mantle source. Hence, we conclude that the two distinct groups not only reflect changes in mantle source composition but may also reflect changes in degree of partial melting.

Using a fractional melting model modified from Bourdon et al. (2005) and Beier et al. (2013) we show that lavas from Condor and Ribeira Funda rifts, and the Ribeirinha Volcano are melting at higher degrees of partial melting between 4 and 8%, compared to 2–4% degree of partial melting at the Central

Fissure Zone and the Caldeira Volcano (**Figure 9**). In agreement with Na_2O, lavas from the Caldeira Volcano display slightly higher degrees of partial melting compared to the Central Fissure Zone (based on lower La/Yb; **Figure 9**). The island of Faial and its submarine ridges, however, are built on a lithosphere with approximately the same thickness of about 30 km, calculated using the 1300°C isotherm of Stein and Stein (1992) and a lithosphere age of about 10 Ma (Cande and Kent, 1995; Luis and Miranda, 2008). Robinson and Wood (1998) have shown that the fractionation of middle Rare Earth Elements (MREE) relative to heavy Rare Earth Elements (HREE) in the melt fraction depends on the amount of residual garnet in the mantle that may be increasing with increasing lithosphere thickness in the oceanic environment. Generally, lavas from Faial contain similar amounts of residual garnet between 4 and 6%. This is in agreement with the fact that the amount of garnet in the residual mantle should not differ significantly within the island and the neighboring rift zones if correlated to lithospheric thickness. Thus, we suggest that the small but notable variability in MREE/HREE ratios reflects variations in their mantle source composition rather than different melting depths, i.e., the lowest Tb/Yb ratios are limited to Condor rift and the Ribeirinha Volcano. We conclude that older lavas from Faial, lavas from Condor and Ribeira Funda rifts and the Ribeirinha Volcano formed at a higher degree of partial melting compared to the younger lavas.

The Origin of Chemical and Isotopic Variations

Changes in source composition may also be accompanied or influenced by changes in the degree of melting, i.e., variably more enriched sources may melt deeper and hence to a larger extent (Phipps Morgan, 2000; Niu et al., 2002; Shorttle et al., 2014). In other volcanic systems (e.g., on Iceland; Maclennan, 2008; Shorttle et al., 2014) neighboring volcanoes which have originated from a single mantle column have distinct correlated trace element and isotope patterns. These differences are probably related to mantle source heterogeneity showing that the source composition and the melting depth are closely linked. Comparatively, a study from the Galapagos Rise (Haase et al., 2011) has shown that differences in major and trace elements and isotopes are the result of different degrees of partial melting of a heterogeneous mantle source. The progressive decrease in degrees of partial melting with time occurred as the rifting of the Galapagos Rise slowed down and finally stopped. As a result incompatible element-enriched mantle lithologies can generate a systematic enrichment in incompatible elements with increasing alkalinity of the melt as they preferentially contribute to melts generated at smaller degrees of partial melting (Haase et al., 2011).

Similar to the Galapagos Rise case, lavas from Faial and adjoining submarine rift zones reflect progressive changes in both their mantle source compositions and degrees of partial melting since ∼1 Ma (from Condor rift to the Central Fissure Zone; **Figure 9**). We suggest that the similarity of both cases, changes in mantle source compositions and the conditions of melting in the Faial lavas result from a process that is linked. The youngest lavas from the Central Fissure Zone (<10 ka) have the most enriched mantle source composition, melting with a lower degree of partial melting compared to the older lavas. Hence, we conclude that the consequence of the progressive decrease in the degree of melting at Faial results in a larger contribution of trace element-enriched mantle lithologies from a heterogenous mantle source characteristic to the Azores melting anomaly (Beier et al., 2018).

Spatial and Temporal Evolution

The large compositional and age differences of the Faial lavas imply that they probably do not derive from one large reservoir beneath the Caldeira Volcano. Although volcanic units with comparable ages tend to be similarly enriched or depleted, they did not evolve along a single fractionation path. The differences in K_2O contents and K_2O/TiO_2 ratios between the Central Fissure Zone and the Caldeira Volcano (**Figures 4B,F**), for example, are too large to be explained by similar liquid lines of descent. Some volcanic systems on Hawaii, i.e., the Kilauea Volcano and the associated Pu'u O'o rift zone (Greene et al., 2013) are geochemically variable and probably derive from one plumbing system. However, the time scales of eruptions with lavas of distinct composition are much shorter (years to decades) compared to Faial. The nature of the periodicity of eruptions on Faial, with short periods of volcanic activity followed by hiatuses of up to several 100 ka (Hildenbrand et al., 2012) rather implies that the compositional differences between distinct volcanic units result from distinct primary magmas and plumbing systems. The younger volcanic units on the island, in particular the Caldeira Volcano, likely cover older units, and in the absence of samples one might speculate that these may form compositional equivalents to the lavas erupted along the submarine rift zones. Thus, we suggest that a model like on Iceland (Gudmundsson, 1995) or Hawaii (Garcia et al., 1996) with a summit reservoir feeding both a central volcano and the rift zones is not applicable for Faial. Instead, the volcanic structures may be comparable to those observed on La Palma where the central volcano and the rift zone formed above distinct plumbing systems (Galipp et al., 2006). Melts feeding the rift zones, e.g., the Central Fissure Zone, ascend from the mantle either directly beneath their locus of eruption or beneath a central volcano, i.e., the Caldeira Volcano. In the latter case, ascending melts would likely stagnate in the uppermost crust, where the base of volcanic edifices and their sedimentary covers have a lower density (Klügel et al., 2005a) and then get laterally transported as sills and dikes into the rift zone. Despite the fact that most samples from the Central Fissure Zone have mafic to intermediate compositions, stagnation and probably further cooling and fractionation beneath the Caldeira Volcano could explain why some samples from the Central Fissure Zone are relatively evolved. However, Zanon and Frezzotti (2013) showed that melts from the subaerial fissure zones have not stagnated significantly during their ascent. In both cases, the effective lateral transport of melts and eruption along fissures are a major process for the development of the rift zones. Elongated rift zones and large volcanic edifices imply that they are internally homogeneous but the distinct geochemical variability between the different rift zones and

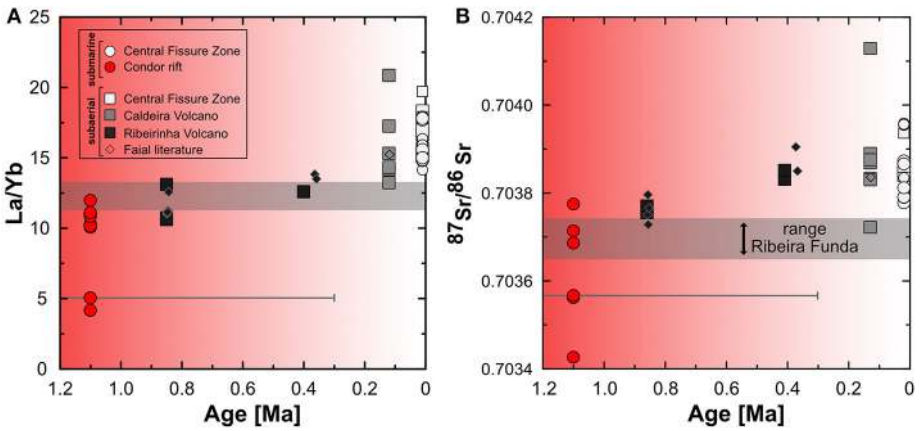

FIGURE 10 | (A) La/Yb and **(B)** $^{87}Sr/^{86}Sr$ vs. absolute (Madeira et al., 1995; Hildenbrand et al., 2012; Beier et al., 2015) and relative ages from seismic profiles of Faial lavas and respective rift zones. La/Yb and $^{87}Sr/^{86}Sr$ ratios display both a progressive decrease in the degree of partial melting and a progressive enrichment of the mantle source compositions. Color gradient schematically illustrates the progressive change in the melting regime from a more depleted mantle source and high degree of partial melting (red) to a more enriched mantle source and a lower degree of partial melting (white) (see also **Figure 11**). Gray area marks the range La/Yb and $^{87}Sr/^{86}Sr$ ratios of the Ribeira Funda rift lavas. Error bars display the analytical variation in Ar-Ar age form the submarine Condor rift. The analytical errors of the other absolute, radiometric ages are smaller than the respective symbols. Note that the lower La/Yb and $^{87}Sr/^{86}Sr$ for those lavas compared to the Caldeira Volcano may indicate that this rift zone is older. Literature data are from Hildenbrand et al. (2014) for La/Yb and $^{87}Sr/^{86}Sr$. The respective ages derive from K-Ar age dating from Hildenbrand et al. (2012) on the same rock specimen like on which the trace element and isotope analysis were carried out. Symbols are maximum radiometric ages from the respective volcanic units.

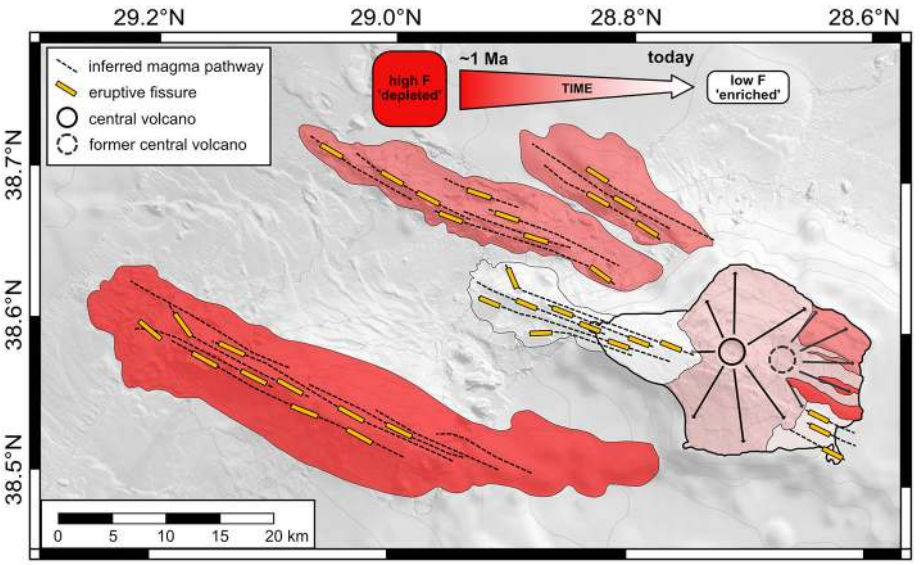

FIGURE 11 | Schematic illustration of the progressive spatial evolution of the conditions of melting and structural features. Note that older lavas with less enriched mantle source compositions at higher degrees of partial melting (F) (dark red colors, large box) occur more widespread than the younger lavas, having more enriched mantle source compositions at lower melting degrees (bright red to white colors, small box). The recent mafic and intermediate volcanic activity on Faial occurs exclusively along narrow rift zones, whereas the older volcanic activity is characterized by both volcanic rift zones and central volcanic edifices. Not to scale.

central volcanoes implies that these systems only show limited interaction.

Combining our chemical observations with the spatial distribution of eruption ages at Faial also provides the possibility to better constrain the temporal evolution of the sources and melting signatures (**Figure 10**). In contrast to the Ribeirinha Volcano forming the oldest volcanism on the island and to some extent the Caldeira Volcano, the youngest mafic and intermediate volcanic activity (<10 ka) on Faial exclusively occurs very localized along rift structures. This may be a result of melt focussing into the rift zones, because the structural features indicate that the tectonic control on youngest

volcanic units becomes stronger, i.e., a preferential formation of volcanic rift zones as opposed to central volcanic edifices. The distribution of lava ages suggests that the youngest mafic and intermediate volcanism occurs on a small area along the Central Fissure Zone and Horta Fissure Zone, whereas the older lavas form both submarine rift zones and large central volcanic edifices and cover large areas (**Figure 11**). The differences in spatial distribution of the volcanic activity correspond to the compositional differences of the groups reflecting different mantle source compositions and degrees of partial melting. This may indicate that the processes leading to compositional variation and eruption style are linked. Hence, the volcanism on Faial appears to become increasingly localized along tectonically controlled lineaments as changes in the melting regime occur.

The similarity of both source and melting signatures in the Faial lavas suggests that this magmatic system is significantly influenced by changes in the melting regime, particularly in the degree of partial melting. A decrease of melting productivity in the upper mantle beneath Faial may be due to a waning of the Azores melting anomaly (O'Neill and Sigloch, 2018). Variability in magmatic productivity is well-documented in other ocean island locations, classically in the alkaline pre-shield, tholeiitic shield and alkaline post-shield phases of Hawaiian volcanism (Clague and Dalrymple, 1987). However, a tholeiitic shield phase is not present in Faial. On Iceland changes in the plume temperature may be responsible for changes in lava compositions (Poore et al., 2011), indicating that geochemical variations in the produced melts are largely driven by changes in the melting regime. However, rift jumps and mantle plume migration may also be responsible for the alkaline volcanic activity of the Snaefellsnes Rift on Iceland (Hardarson et al., 1997), indicating that changes in both tectonic and magmatic processes may variably contribute to changes in the lava compositions. In the eastern Azores Plateau the successive jumps of the Terceira Rift (Gente et al., 2003; Vogt and Jung, 2004) to its present position may additionally support the decreasing degrees of partial melting beneath Faial. However, the position of the triple junction in the Azores remains unclear and may be treated as a diffuse plate boundary situated in the vicinity of the area west of Faial and/or Graciosa (Miranda et al., 2014). Noble gas isotopes and melting models suggest that a deep mantle plume may be located beneath Terceira (Moreira et al., 1999; Bourdon et al., 2005), some 150 km north-east of Faial, whereas geophysical models suggest the plume beneath Faial (Yang et al., 2006). However, our data suggest that the melt supply beneath Faial decreases toward the youngest volcanism. We conclude that the progressive changes in the melting regime, the composition of melts and their spatial distribution reflect changes in the plate tectonic regime and mantle plume upwelling. Even though the Azores case with an extensional tectonic regime above a (wet) melting anomaly may be treated as a rather unique case, these observations may also be applicable to other (intraplate) settings where both significant tectonic stresses and magmatism are present, e.g., in the Canary Islands or on Iceland. We note however, that the Canary Islands may contain less of a plate tectonic component whereas the Iceland volcanic systems combined a much stronger plume signal with a true spreading movement.

SUMMARY AND CONCLUSIONS

The island of Faial and the western adjoining submarine rift zones have undergone a complex volcano-tectonic evolution. We use new geophysical, high resolution bathymetric, geochemical, and Sr-Nd-Pb isotope data combined with published ages to expand existing models covering the volcanic and tectonic evolution of the island and its submarine rift zones in the Azores. Much of the volcanism related to Faial occurs below sea level, covering a similar spatial extent compared to the subaerial volcanism. The formation of four WNW-ESE oriented narrow submarine structural and magmatic features since ∼1 Ma together with the formation of the Pedro Miguel graben some 400 ka ago both likely resulting from extensional stresses, show that lithospheric extension is an important process during the evolution of the subaerial and submarine volcanic structures. We suggest that dikes efficiently transport melts along the volcanic rift zones at Faial over length scales of >12 km while plumbing systems parallel to the rift axes are distinct over a similar length scale, e.g., the distance between Capelinhos and Condor rifts. The fact that the orientation of the rift zones and other structural features related to tectonic stresses on Faial have generally not changed since their formation ∼1 Ma shows that the regional tectonic stress field has not changed significantly during the evolution of the island. Lavas from Faial and its respective submarine rift zones, however, display a regular spatial distribution in both compositional signatures (mantle source compositions and degree of partial melting) and ages of eruption (**Figures 10**, **11**). The older lavas from 1.1 Ma to ∼400 ka formed by higher degrees of partial melting from a more depleted mantle source and cover a larger area. The younger volcanic activity forms by smaller degrees of partial melting from a more enriched source. We suggest that the degree of partial melting decreases progressively toward the youngest volcanism resulting in increasingly enriched magmas, largely sampling the enriched mantle sources as they preferentially contribute to small degree melts. As melt supply decreases, volcanism appears to become increasingly localized along tectonically controlled (active and non-active) lineaments in the last 10 ka exclusively erupting along fissures, alignments of elongated cones and dikes. Hence, mafic and intermediate melts erupted during the youngest volcanic activity on Faial focus along single rift zones, whereas the old volcanism occurs more widespread. The compositional and age differences between the central volcanic edifices and the rift zones suggest that lavas feeding these systems do not derive from one shallow magma reservoir and rather derived from different plumbing systems. Our study demonstrates the importance of detailed geochemical investigations of ocean islands that are strongly influenced by tectonic stresses and their potential to disentangle how changes in the melting regime may be reflected in the structural features of volcanic bodies and their spatial distribution. A continuous change in divergent

plate movements may affect the melt formation and supply from the mantle.

AUTHOR CONTRIBUTIONS

All authors were involved in the data acquisition. CB was chief scientist on cruise M128 and was responsible for sampling of volcanic rocks during cruise M113 and on Faial. CH was chief scientist on cruise M113 and responsible for the seismic data acquisition, selection of sampling localities and their interpretation. RR prepared and analyzed the rock samples, wrote the manuscript and designed the manuscript. All authors discussed and contributed to the final manuscript.

ACKNOWLEDGEMENTS

We acknowledge help and support from captains M. Schneider and J. F. Schubert, crews and scientists during M113 and M128 for their invaluable, friendly support during the—at times difficult—operations. A special thanks to M. Regelous for support in the Erlangen clean laboratories. We acknowledge the constructive and helpful reviews by D. A. Neave, V. Acocella and R. Gertisser, and constructive and helpful annotations and editorial handling by A. Pimentel. We thank K. Knevels for providing help with the geophysical data. We thank V.H. Forjaz, Peter and Basalto for their support during the field work on the islands. RR thanks M.V. Schoenhofen, A. Eberts, C. Kraft, and B. Held for inspiration and support during this study. This study was funded by the Deutsche Forschungsgemeinschaft (DFG grant BE4459/9-1).

SUPPLEMENTARY MATERIAL

The Supplementary Material for this article can be found online at: https://www.frontiersin.org/articles/10.3389/feart.2018.00078/full#supplementary-material

REFERENCES

Adam, J., and Green, T. (2006). Trace element partitioning between mica- and amphibole-bearing garnet lherzolite and hydrous basanitic melt: 1. experimental results and the investigation of controls on partitioning behaviour. *Contrib.Mineral. Petrol.* 152, 1–17. doi: 10.1007/s00410-006-0085-4

Beier, C., Bach, W., Blum, M., Cerqueira, T. S., da Costa, I. R., Ferreira, P. J., et al. (2017a). *Azores Plateau - Cruise No. M128 - July 02, 2016 - July 27, 2016 - Ponta Delgada (Portugal) - Ponta Delgada (Portugal). METEOR-Berichte. DFG-Senatskommission für Ozeanographie*, 41

Beier, C., Haase, K. M., and Abouchami, W. (2015). Geochemical and geochronological constraints on the evolution of the Azores Plateau. *Geol. Soc. Am.Spec. Pap.* 511, 27–55. doi: 10.1130/2015.2511(02)

Beier, C., Haase, K. M., Abouchami, W., Krienitz, M. S., and Hauff, F. (2008). Magma genesis by rifting of oceanic lithosphere above anomalous mantle: Terceira Rift, Azores. *Geochem. Geophys. Geosyst.* 9:Q12013. doi: 10.1029/2008GC002112

Beier, C., Haase, K. M., and Brandl, P. A. (2018). "Melting and mantle sources in the Azores," in *Volcanoes of the Azores: Revealing the Geological Secrets of the Central Northern Atlantic Islands,* eds U. Kueppers and C. Beier (Heidelberg: Springer), 251–280.

Beier, C., Haase, K. M., Brandl, P. A., and Krumm, S. H. (2017b). Primitive andesites from the Taupo Volcanic Zone formed by magma mixing. *Contrib. Miner. Petrol.* 172:33. doi: 10.1007/s00410-017-1354-0

Beier, C., Haase, K. M., and Hansteen, T. H. (2006). Magma evolution of the Sete Cidades volcano, São Miguel, Azores. *J. Petrol.* 47, 1375–1411. doi: 10.1093/petrology/egl014

Beier, C., Haase, K. M., and Turner, S. P. (2012). Conditions of melting beneath the Azores. *Lithos* 144, 1–11. doi: 10.1016/j.lithos.2012.02.019

Beier, C., Mata, J., Stöckhert, F., Mattielli, N., Brandl, P. A., Madureira, P., et al. (2013). Geochemical evidence for melting of carbonated peridotite on Santa Maria Island, Azores. *Contrib. Mineral. Petrol.* 165, 823–841. doi: 10.1007/s00410-012-0837-2

Beier, C., Stracke, A., and Haase, K. M. (2007). The peculiar geochemical signatures of São Miguel (Azores) lavas: metasomatised or recycled mantle sources? *Earth Planet. Sci. Lett.* 259, 186–199.doi: 10.1016/j.epsl.2007.04.038

Bonatti, E. (1990). Not so hot "hot spots" in the oceanic mantle. *Science* 250, 107–111. doi: 10.1126/science.250.4977.107

Bourdon, B., Turner, S. P., and Ribe, N. M. (2005). Partial melting and upwelling rates beneath the Azores from a U-series isotope perspective. *Earth Planet. Sci. Lett.* 239, 42–56. doi: 10.1016/j.epsl.2005.08.008

Brandl, P. A., Beier, C., Regelous, M., Abouchami, W., Haase, K. M., Garbe-Schönberg, D., et al. (2012). Volcanism on the flanks of the east pacific rise: quantitative constraints on mantle heterogeneity and melting processes. *Chem. Geol.* 298, 41–56. doi: 10.1016/j.chemgeo.2011.12.015

Cande, S. C., and Kent, D. V. (1995). Revised calibration of the geomagnetic polarity timescale for the Late Cretaceous and Cenozoic. *J. Geophys. Res. Solid Earth* 100, 6093–6095. doi: 10.1029/94JB03098

Cannat, M., Briais, A., Deplus, C., Escartin, J., Georgen, J., Lin, J. et al. (1999). Mid-Atlantic Ridge–Azores hotspot interactions: along-axis migration of a hotspot-derived event of enhanced magmatism 10 to 4 Ma ago. *Earth Planet. Sci. Lett.* 173, 257–269. doi: 10.1016/S0012-821X(99)00234-4

Chovelon, P. (1982). *Évolution Volcanotectonique des Iles de Faial et de Pico*. Thesis Univ., Paris-Sud, Orsay, 186.

Clague, D. A., and Dalrymple, G. B. (1987). The Hawaiian-Emperor volcanic chain. part I. Geologic evolution. *Volcanism Hawaii* 1, 5–54.

Cole, P. D., Guest, J. E., Duncan, A. M., and Pacheco, J.-M. (2001). Capelinhos 1957–1958, Faial, Azores: deposits formed by an emergent surtseyan eruption. *Bull. Volcanol.* 63:204. doi: 10.1007/s004450100136

Compston, W., and Oversby, V. M. (1969). Lead isotopic analysis using a double spike. *J. Geophys. Res.* 74, 4338–4348.

Daly, G. E., Widom, E., and Franca, Z. (2012). Evolution of silicic magmas and the origin of the Daly Gap at Santa Barbara volcano, Terceira, Azores. *Miner. Mag.* 76, 1613–1674.

Demande, J., Fabriol, R., Gérard, A., and Iundt, F. (1982). *Prospection Géothermique des Iles de Faial et Pico (Açores). 82SGN003GTH.* Bureau de recherches géologiques et minières, Orléans.

Dias, N. A., Matias, L., Lourenço, N., Madeira, J., Carrilho, F., and Gaspar, J. L. (2007). Crustal seismic velocity structure near Faial and Pico Islands (AZORES), from local earthquake tomography. *Tectonophysics* 445, 301–317. doi: 10.1016/j.tecto.2007.09.001

Di Chiara, A., Speranza, F., Porreca, M., Pimentel, A., D'Ajello Caracciolo, F., and Pacheco, J. (2014). Constraining chronology and time-space evolution of Holocene volcanic activity on the Capelo Peninsula (Faial Island, Azores): the paleomagnetic contribution. *Bulletin* 126, 1164–1180. doi: 10.1130/B30933.1

Dosso, L., Bougault, H., Langmuir, C., Bollinger, C., Bonnier, O., and Etoubleau, J. (1999). The age and distribution of mantle heterogeneity along the Mid-Atlantic Ridge (31–41 N). *Earth Planet. Sci. Lett.* 170, 269–286. doi: 10.1016/S0012-821X(99)00109-0

Elliott, T., Blichert-Toft, J., Heumann, A., Koetsier, G., and Forjaz, V. (2007). The origin of enriched mantle beneath Sao Miguel, Azores. *Geochim. Cosmochim. Acta* 71, 219–240. doi: 10.1016/j.gca.2006.07.043

Feraud, G., Kaneoka, I., and Allègre, C. J. (1980). K/Ar ages and stress pattern in the Azores: geodynamic implications. *Earth Planet. Sci. Lett.* 46, 275–286. doi: 10.1016/0012-821X(80)90013-8

Fernandes, R. M. S., Miranda, J. M., Catalão, J., Luis, J. F., Bastos, L., and Ambrosius, B. A. C. (2002). Coseismic displacements of the MW = 6.1, July 9, 1998, Faial earthquake (Azores, North Atlantic). *Geophys. Res. Lett.* 29, 21.1–21.4. doi: 10.1029/2001GL014415

Fontiela, J., Oliveira, C. S., and Rosset, P. (2018). "Characterisation of seismicity of the azores archipelago: an overview of historical events and a detailed analysis for the period 2000–2012," in *Volcanoes of the Azores: Revealing the Geological Secrets of the Central Northern Atlantic Islands*, eds U. Kueppers and C. Beier (Heidelberg: Springer), 127–153

Freund, S., Beier, C., Krumm, S., and Haase, K. M. (2013). Oxygen isotope evidence for the formation of andesitic–dacitic magmas from the fast-spreading Pacific–Antarctic Rise by assimilation–fractional crystallisation. *Chem. Geol.* 347, 271–283. doi: 10.1016/j.chemgeo.2013.04.013

Galipp, K., Klügel, A., and Hansteen, T. H. (2006). Changing depths of magma fractionation and stagnation during the evolution of an oceanic island volcano: La Palma (Canary Islands). *J. Volcanol. Geotherm. Res.* 155, 285–306. doi: 10.1016/j.jvolgeores.2006.04.002

Garcia, M. O., Rhodes, J. M., Trusdell, F. A., and Pietruszka, A. J. (1996). Petrology of lavas from the Puu Oo eruption of Kilauea Volcano: III. The Kupaianaha episode (1986–1992). *Bull. Volcanol.* 58, 359–379. doi: 10.1007/s004450050145

Gente, P., Dyment, J., Maia, M., and Goslin, J. (2003). Interaction between the Mid-Atlantic Ridge and the Azores hot spot during the last 85 Myr: Emplacement and rifting of the hot spot-derived plateaus. *Geochem. Geophys. Geosyst.* 4:8514. doi: 10.1029/2003GC000527

Green, T. H., Blundy, J. D., Adam, J., and Yaxley, G. M. (2000). SIMS determination of trace element partition coefficients between garnet, clinopyroxene and hydrous basaltic liquids at 2–7.5 GPa and 1080–1200°C. *Lithos* 53, 165–187. doi: 10.1016/S0024-4937(00)00023-2

Greene, A. R., Garcia, M. O., Pietruszka, A. J., Weis, D., Marske, J. P., Vollinger, M. J., et al. (2013). Temporal geochemical variations in lavas from Kilauea's Pu 'u 'O 'o eruption (1983–2010): cyclic variations from melting of source heterogeneities. *Geochem. Geophys. Geosyst.* 14, 4849–4873. doi: 10.1002/ggge.20285

Grimison, N., and Chen, W.-P. (1988). Source mechanisms of four recent earthquakes along the Azores-Gibraltar plate boundary. *Geophys. J.* 92, 391–401.

Gudmundsson, A. (1995). Infrastructure and mechanics of volcanic systems in Iceland. *J. Volcanol. Geotherm. Res.* 64, 1–2. doi: 10.1016/0377-0273(95)92782-Q

Gudmundsson, A., Lecoeur, N., Mohajeri, N., and Thordarson, T. (2014). Dike emplacement at Bardarbunga, Iceland, induces unusual stress changes, caldera deformation, and earthquakes. *Bull. Volcanol.* 76:869. doi: 10.1007/s00445-014-0869-8

Gudmundsson, M. T., Jónsdóttir, K., Hooper, A., Holohan, E. P., Halldórsson, S. A., Ófeigsson, B. G., et al. (2016). Gradual caldera collapse at Bárdarbunga volcano, Iceland, regulated by lateral magma outflow. *Science* 353:aaf8988. doi: 10.1126/science.aaf8988

Haase, K. M., and Beier, C. (2003). Tectonic control of ocean island basalt sources on São Miguel, Azores? *Geophys. Res. Lett.* 30. doi: 10.1029/2003GL017500

Haase, K. M., Beier, C., Regelous, M., Rapprich, V., and Renno, A. (2017). Spatial variability of source composition and petrogenesis in rift and rift flank alkaline lavas from the Eger Rift, Central Europe. *Chem. Geol.* 455, 304–314. doi: 10.1016/j.chemgeo.2016.11.003

Haase, K. M., Regelous, M., Duncan, R. A., Brandl, P. A., Stroncik, N., and Grevemeyer, I. (2011). Insights into mantle composition and mantle melting beneath mid-ocean ridges from postspreading volcanism on the fossil Galapagos Rise. *Geochem. Geophys. Geosyst.* 12:Q0AC11. doi: 10.1029/2010GC003482

Halliday, A. N., Lee, D.-C., Tommasini, S., Davies, G. R., Paslick, C. R., Fitton, J. G., et al. (1995). Incompatible trace elements in OIB and MORB and source enrichment in the sub-oceanic mantle. *Earth Planet. Sci. Lett.* 133, 379–395.

Hardarson, B. S., Fitton, J. G., Ellam, R. M., and Pringle, M. S. (1997). Rift relocation — A geochemical and geochronological investigation of a palaeo-rift in northwest Iceland. *Earth Planet. Sci. Lett.* 153, 181–196.

Hawkesworth, C., Norry, M., Roddick, J., and Vollmer, R. (1979). $^{143}Nd/^{144}Nd$ and $^{87}Sr/^{86}Sr$ ratios from the Azores and their significance in LIL-element enriched mantle. *Nature* 280, 28–31.

Hildenbrand, A., Madureira, P., Marques, F. O., Cruz, I., Henry, B., and Silva, P. (2008). Multi-stage evolution of a sub-aerial volcanic ridge over the last 1.3 Myr: S. Jorge Island, Azores Triple Junction. *Earth Planet. Sci. Lett.* 273, 289–298. doi: 10.1016/j.epsl.2008.06.041

Hildenbrand, A., Marques, F. O., Costa, A. C. G., Sibrant, A. L. R., Silva, P. F., Henry, B., et al. (2012). Reconstructing the architectural evolution of volcanic islands from combined K/Ar, morphologic, tectonic, and magnetic data: the Faial Island example (Azores). *J. Volcanol. Geotherm. Res.* 241, 39–48. doi: 10.1016/j.jvolgeores.2012.06.019

Hildenbrand, A., Weis, D., Madureira, P., and Marques, F. O. (2014). Recent plate re-organization at the Azores Triple Junction: evidence from combined geochemical and geochronological data on Faial, S. Jorge and Terceira volcanic islands. *Lithos* 210, 27–39. doi: 10.1016/j.lithos.2014.09.009

Hofmann, A. (1997). Mantle geochemistry: the message from oceanic volcanism. *Nature* 385, 219–229.

Hofmann, A. (2003). Sampling mantle heterogeneity through oceanic basalts: isotopes and trace elements. *Treatise Geochem.* 2:568. doi: 10.1016/B0-08-043751-6/02123-X

Hübscher, C., Beier, C., Al-Hseinat, M., Batista, L., Blum, M., Bobsin, M., et al. (2016). *Azores Plateau - Cruise No. M113/1 - December 29, 2014 - January 22, 2015 - Ponta Delgada (Portugal) - Ponta Delgada (Portugal)*. METEOR-Berichte 31.

Hübscher, C., and Gohl, K. (2014). *Reflection/Refraction Seismology*. Encyclopedia of Marine Geosciences. New York, NY: Springer.

Klein, E. M., and Langmuir, C. H. (1987). Global correlations of ocean ridge basalt chemistry with axial depth and crustal thickness. *J. Geophys. Res. Solid Earth* 92, 8089–8115.

Klügel, A., Hansteen, T. H., and Galipp, K. (2005a). Magma storage and underplating beneath Cumbre Vieja volcano, La Palma (Canary Islands). *Earth Planet. Sci. Lett.* 236, 211–226. doi: 10.1016/j.epsl.2005.04.006

Klügel, A., Walter, T. R., Schwarz, S., and Geldmacher, J. (2005b). Gravitational spreading causes en-echelon diking along a rift zone of Madeira Archipelago: an experimental approach and implications for magma transport. *Bull. Volcanol.* 68, 37–46. doi: 10.1007/s00445-005-0418-6

Krause, D. C., and Watkins, N. D. (1970). North Atlantic Crustal Genesis in the Vicinity of the Azores. *Geophys. J. R. Astron. Soc.* 19, 261–283.

Larrea, P., França, Z., Widom, E., and Lago, M. (2018). "Petrology of the Azores Islands," in *Volcanoes of the Azores: Revealing the Geological Secrets of the Central Northern Atlantic Islands*,eds U. Kueppers and C. Beier (Heidelberg: Springer), 197–249.

Larrea, P., Wijbrans, J. R., Galé, C., Ubide, T., Lago, M., França, Z., et al. (2014). 40Ar/39Ar constraints on the temporal evolution of Graciosa Island, Azores (Portugal). *Bull. Volcanol.* 76:796. doi: 10.1007/s00445-014-0796-8

Le Maitre, R. W., Bateman, P., Dudek, A., Keller, J., LeBas, M. J., Sabine, P.A., et al. (1989). *A Classification of Igneous Rocks and Glossary of Terms*. Oxford: Blackwell.

Luis, J. F., and Miranda, J. M. (2008). Reevaluation of magnetic chrons in the North Atlantic between 35 degrees N and 47 degrees N: implications for the formation of the Azores Triple Junction and associated plateau. *J. Geophys. Res. Solid Earth* 113:B10105. doi: 10.1029/2007JB005573

Luis, J. F., Miranda, J. M., Galdeano, A., Patriat, P., Rossignol, J. C., and Victor, L. A. M. (1994). The Azores triple junction evolution since 10 Ma from an aeromagnetic survey of the Mid-Atlantic Ridge. *Earth Planet. Sci. Lett.* 125, 439–459.

Luis, J., Miranda, J., Galdeano, A., and Patriat, P. (1998). Constraints on the structure of the Azores spreading center from gravity data. *Mar. Geophys. Res.* 20, 157–170.

Maclennan, J. (2008). Lead isotope variability in olivine-hosted melt inclusions from Iceland. *Geochim. Cosmochim. Acta* 72, 4159–4176. doi: 10.1016/j.gca.2008.05.034

Madeira, J. (1998). *Estudos de Neotectónica nas Ilhas do Faial, Pico e S. Jorge: Uma Contribuição para o Conhecimento Geodinâmico da Junção Tripla dos Açores*. Ph.D. thesis, Lisbon University, Lisbon.

Madeira, J., Soares, A. M., Da Silveira, A. B., and Serralheiro, A. (1995). Radiocarbon dating recent volcanic activity on Faial Island (Azores). *Radiocarbon* 37, 139–147.

Madureira, P., Mata, J., Mattielli, N., Queiroz, G., and Silva, P. (2011). Mantle source heterogeneity, magma generation and magmatic evolution at Terceira

Island (Azores archipelago): constraints from elemental and isotopic (Sr, Nd, Hf, and Pb) data. *Lithos* 126, 402–418. doi: 10.1016/j.lithos.2011.07.002

Marques, F., Catalão, J., Hildenbrand, A., Costa, A., and Dias, N. (2014). The 1998 Faial earthquake, Azores: evidence for a transform fault associated with the Nubia–Eurasia plate boundary? *Tectonophysics* 633, 115–125. doi: 10.1016/j.tecto.2014.06.024

Marques, F. O., Catalão, J. C., DeMets, C., Costa, A. C. G., and Hildenbrand, A. (2013). GPS and tectonic evidence for a diffuse plate boundary at the Azores Triple Junction. *Earth Planet. Sci. Lett.* 381, 177–187. doi: 10.1016/j.epsl.2013.08.051

Matias, L., Dias, N. A., Morais, I., Vales, D., Carrilho, F., Madeira, J., et al. (2007). The 9th of July 1998 Faial Island (Azores, North Atlantic) seismic sequence. *J. Seismol.* 11, 275–298. doi: 10.1007/s10950-007-9052-4

McDonough, W. F., and Sun, S.-S. (1995). The composition of the Earth. *Chem. Geol.* 120, 223–253.

McKenzie, D., and Bickle, M. J. (1988). The volume and composition of melt generated by extension of the lithosphere. *J. Petrol.* 29, 625–679.

Miranda, J., Luis, J., Lourenço, N., and Goslin, J. (2014). Distributed deformation close to the Azores Triple "Point". *Mar. Geol.* 355, 27–35. doi: 10.1016/j.margeo.2014.05.006

Miranda, J. M., Luis, J. F., and Lourenço, N. (2018). "The tectonic evolution of the Azores based on magnetic data," in *Volcanoes of the Azores: Revealing the Geological Secrets of the Central Northern Atlantic Islands,* eds U. Kueppers and C. Beier (Heidelberg: Springer), 89–100

Miranda, J. M., Victor, L. A. M., Simões, J. Z., Luis, J. F., Matias, L., Shimamura, H., et al. (1998). Tectonic setting of the Azores Plateau deduced from a OBS survey. *Mar. Geophys. Res.* 20, 171–182.

Moreira, M. A., Madureira, P., and Mata, J. (2018). "Noble gas constraints on the origin of the Azores hotspot," in *Volcanoes of the Azores: Revealing the Geological Secrets of the Central Northern Atlantic Islands*, eds U. Kueppers and C. Beier (Heidelberg: Springer), 281–299.

Moreira, M., Doucelance, R., Kurz, M. D., Dupré, B., and Allègre, C. J. (1999). Helium and lead isotope geochemistry of the Azores Archipelago. *Earth Planet. Sci. Lett.* 169, 189–205.

Morgan, J. P. (1987). Melt migration beneath mid-ocean spreading centers. *Geophys. Res. Lett.* 14, 1238–1241.

Morgan, W. J. (1971). Convection plumes in the lower mantle. *Nature* 230, 42–43.

Neave, D. A., Passmore, E., Maclennan, J., Fitton, G., and Thordarson, T. (2013). Crystal–melt relationships and the record of deep mixing and crystallization in the ad 1783 laki eruption, Iceland. *J. Petrol.* 54, 1661–1690. doi: 10.1093/petrology/egt027

Niu, Y., Regelous, M., Wendt, I. J., Batiza, R., and O'Hara, M. J. (2002). Geochemistry of near-EPR seamounts: importance of source vs. process and the origin of enriched mantle component. *Earth Planet. Sci. Lett.* 199, 327–345. doi: 10.1016/S0012-821X(02)00591-5

O'Neill, C., and Sigloch, K. (2018). "Crust and mantle structure beneath the Azores Hotspot—Evidence from geophysics," in *Volcanoes of the Azores: Revealing the Geological Secrets of the Central Northern Atlantic Islands*, eds U. Kueppers and C. Beier (Heidelberg: Springer), 71–87.

Pacheco, J. (2001). *Processos Associados ao Desenvolvimento de Erupções Vulcânicas Hidromagmáticas na Ilha do Faial e sua Interpretação Numa Perspectiva de Avaliação do Hazard e Minimização do Risco*. Ph.D. Thesis, University of the Azores.

Paquet, F., Dauteuil, O., Hallot, E., and Moreau, F. (2007). Tectonics and magma dynamics coupling in a dyke swarm of Iceland. *J. Struct. Geol.* 29, 1477–1493. doi: 10.1016/j.jsg.2007.06.001

Phipps Morgan, J. (2000). Isotope topology of individual hotspot basalt arrays: mixing curves or melt extraction trajectories? *Geochem. Geophys. Geosyst.* 1:1003. doi: 10.1029/1999GC000004

Pimentel, A., Pacheco, J., and Self, S. (2015). The ∼1000-years BP explosive eruption of Caldeira Volcano (Faial, Azores): the first stage of incremental caldera formation. *Bull. Volcanol.* 77:42. doi: 10.1007/s00445-015-0930-2

Poore, H., White, N., and Maclennan, J. (2011). Ocean circulation and mantle melting controlled by radial flow of hot pulses in the Iceland plume. *Nat. Geosci.* 4:558. doi: 10.1038/NGEO1161

Prytulak, J., and Elliott, T. (2007). TiO2 enrichment in ocean island basalts. *Earth Planet. Sci. Lett.* 263, 388–403. doi: 10.1016/j.epsl.2007.09.015

Quartau, R., and Mitchell, N. C. (2013). Comment on "Reconstructing the architectural evolution of volcanic islands from combined K/Ar, morphologic, tectonic, and magnetic data: The Faial Island example (Azores)" by Hildenbrand et al. (2012) [J. Volcanol. Geotherm. Res. 241–242 (2012) 39–48]. *J. Volcanol. Geotherm. Res.* 255, 124–126. doi: 10.1016/j.jvolgeores.2012.12.020

Quartau, R., Tempera, F., Mitchell, N. C., Pinheiro, L. M., Duarte, H., Brito, P. O., et al. (2012). Morphology of the Faial Island shelf (Azores): the interplay between volcanic, erosional, depositional, tectonic and mass-wasting processes. *Geochem. Geophys. Geosyst.* 13:Q04012. doi: 10.1029/2011GC003987

Ramalho, R. S., Helffrich, G., Madeira, J., Cosca, M., Thomas, C., Quartau, R., et al. (2017). Emergence and evolution of Santa Maria Island (Azores)—The conundrum of uplifted islands revisited. *Bulletin* 129, 372–390. doi: 10.1130/B31538.1

Robinson, J. A. C., and Wood, B. J. (1998). The depth of the spinel to garnet transition at the peridotite solidus. *Earth Planet. Sci. Lett.* 164, 277–284.

Roeder, P., and Emslie, R. (1970). Olivine-liquid equilibrium. *Contrib. Mineral. Petrol.* 29, 275–289.

Schilling, J.-G. (1975). Azores mantle blob: rare-earth evidence. *Earth Planet. Sci. Lett.* 25, 103–115.

Schilling, J.-G., Bergeron, M., Evans, R., and Smith, J. (1980). Halogens in the mantle beneath the north atlantic [and discussion]. *Philos. Trans. R. Soc. Lond. A Math. Phys. Eng. Sci.* 297, 147–178.

Schwarz, S., Klugel, A., van den Bogaard, P., and Geldmacher, J. (2005). Internal structure and evolution of a volcanic rift system in the eastern North Atlantic: the Desertas rift zone, Madeira archipelago. *J. Volcanol. Geotherm. Res.* 141, 123–155. doi: 10.1016/j.jvolgeores.2004.10.002

Shorttle, O., Maclennan, J., and Lambart, S. (2014). Quantifying lithological variability in the mantle. *Earth Planet. Sci. Lett.* 395, 24–40. doi: 10.1016/j.epsl.2014.03.040

Shorttle, O., Maclennan, J., and Piotrowski, A. M. (2013). Geochemical provincialism in the Iceland plume. *Geochim. Cosmochim. Acta* 122, 363–397. doi: 10.1016/j.gca.2013.08.032

Sibrant, A. L. R., Hildenbrand, A., Marques, F. O., and Costa, A. C. G. (2015). Volcano-tectonic evolution of the Santa Maria Island (Azores): implications for paleostress evolution at the western Eurasia–Nubia plate boundary. *J. Volcanol. Geotherm. Res.* 291, 49–62. doi: 10.1016/j.jvolgeores.2014.12.017

Sibrant, A. L. R., Marques, F. O., Hildenbrand, A., Boulesteix, T., Costa, A. C. G., and Catalão, J. (2016). Deformation in a hyperslow oceanic rift: insights from the tectonics of the São Miguel Island (Terceira Rift, Azores). *Tectonics* 35, 425–446. doi: 10.1002/2015TC003886

Sibrant, A., Marques, F., and Hildenbrand, A. (2014). Construction and destruction of a volcanic island developed inside an oceanic rift: Graciosa Island, Terceira Rift, Azores. *J. Volcanol. Geotherm. Res.* 284, 32–45. doi: 10.1016/j.jvolgeores.2014.07.014

Sigmundsson, F., Hooper, A., Hreinsdóttir, S., Vogfjörd, K. S., Ófeigsson, B. G., and Heimisson, E.R. (2014). Segmented lateral dyke growth in a rifting event at Bárð*arbunga volcanic system, Iceland. *Nature* 517, 191–195. doi: 10.1038/nature14111

Stein, C. A., and Stein, S. (1992). A model for the global variation in oceanic depth and heat flow with lithospheric age. *Nature* 359, 123–129.

Stracke, A. (2012). Earth's heterogeneous mantle: a product of convection-driven interaction between crust and mantle. *Chem. Geol.* 330–331, 274–299. doi: 10.1016/j.chemgeo.2012.08.007

Sun, S.-S., and McDonough, W.-S. (1989). Chemical and isotopic systematics of oceanic basalts: implications for mantle composition and processes. *Geol. Soc. Lond. Spec. Publ.* 42, 113–345.

Tempera, F., Hipólito, A., Madeira, J., Vieira, S., Campos, A. S., and Mitchell, N. C. (2013). Condor seamount (Azores, NE Atlantic): a morpho-tectonic interpretation. *Deep Sea Res. Part II Top. Stud. Oceanogr.* 98, 7–23. doi: 10.1016/j.dsr2.2013.09.016

Tibaldi, A., Bonali, F. L., and Corazzato, C. (2014). The diverging volcanic rift system. *Tectonophysics* 611, 94–113. doi: 10.1016/j.tecto.2013.11.023

Trippanera, D., Porreca, M., Ruch, J., Pimentel, A., Acocella, V., Pacheco, J., et al. (2014). Relationships between tectonics and magmatism in a transtensive/transform setting: an example from Faial Island (Azores, Portugal). *GSA Bull.* 126, 164–181. doi: 10.1130/B30758.1

Turner, S., Hawkesworth, C., Rogers, N., and King, P. (1997). U-Th isotope disequilibria and ocean island basalt generation in the Azores. *Chem. Geol.* 139, 145–164.

Villemant, B., Jaffrezic, H., Joron, J.-L., and Treuil, M. (1981). Distribution coefficients of major and trace elements; fractional crystallization in the alkali basalt series of Chaine des Puys (Massif Central, France). *Geochim. Cosmochim. Acta* 45, 1997–2016.

Vogt, P., and Jung, W. (2004). The Terceira Rift as hyper-slow, hotspot-dominated oblique spreading axis: a comparison with other slow-spreading plate boundaries. *Earth Planet. Sci. Lett.* 218, 77–90. doi: 10.1016/S0012-821X(03)00627-7

Vogt, P. R., and Jung, W.-Y. (2018). "The "Azores Geosyndrome" and plate tectonics: research history, synthesis, and unsolved puzzles," in *Volcanoes of the Azores: Revealing the Geological Secrets of the Central Northern Atlantic Islands*, eds U. Kueppers and C. Beier (Heidelberg: Springer), 27–56.

Weiß, B. J., Hübscher, C., and Lüdmann, T. (2015a). The tectonic evolution of the southeastern Terceira Rift/São Miguel region (Azores). *Tectonophysics* 654, 75–95. doi: 10.1016/j.tecto.2015.04.018

Weiß, B. J., Hübscher, C., Wolf, D., and Lüdmann, T. (2015b). Submarine explosive volcanism in the southeastern Terceira Rift/São Miguel region (Azores). *J. Volcanol. Geotherm. Res.* 303, 79–91. doi: 10.1016/j.jvolgeores.2015.07.028

White, W. M., Schilling, J. G., and Hart, S. R. (1976). Evidence for Azores mantle plume from strontium isotope geochemistry of Central North-Atlantic. *Nature* 263, 659–663.

Widom, E., Carlson, R., Gill, J., and Schmincke, H.-U. (1997). Th–Sr–Nd–Pb isotope and trace element evidence for the origin of the Sao Miguel, Azores, enriched mantle source. *Chem. Geol.* 140, 49–68.

Woelki, D., Haase, K. M., Schoenhofen, M. V., Beier, C., Regelous, M., Krumm, S. H., et al. (2018). Evidence for melting of subducting carbonate-rich sediments in the western Aegean Arc. *Chem. Geol.* 483, 463–473. doi: 10.1016/j.chemgeo.2018.03.014

Yang, T., Shen, Y., van der Lee, S., Solomon, S. C., and Hung, S.-H. (2006). Upper mantle structure beneath the Azores hotspot from finite-frequency seismic tomography. *Earth Planet. Sci. Lett.* 250, 11–26. doi: 10.1016/j.epsl.2006.07.031

Zanon, V., and Frezzotti, M. L. (2013). Magma storage and ascent conditions beneath Pico and Faial islands (Azores archipelago): a study on fluid inclusions. *Geochem. Geophys. Geosyst.* 14, 3494–3514. doi: 10.1002/ggge.20221

Zanon, V., Kueppers, U., Pacheco, J. M., and Cruz, I. (2013). Volcanism from fissure zones and the Caldeira central volcano of Faial Island, Azores archipelago: geochemical processes in multiple feeding systems. *Geol. Mag.* 150, 536–555. doi: 10.1017/S0016756812000702

Zindler, A., and Hart, S. (1986). Chemical geodynamics. *Annu. Rev. Earth Planet. Sci.* 14, 493–571.

Conflict of Interest Statement: The authors declare that the research was conducted in the absence of any commercial or financial relationships that could be construed as a potential conflict of interest.